

TRIM37 is a new histone H2A ubiquitin ligase and breast cancer oncoprotein

Sanchita Bhatnagar^{1,2}, Claude Gazin³, Lynn Chamberlain^{1,2}, Jianhong Ou², Xiaochun Zhu^{1,2}, Jogender S. Tushir⁴, Ching-Man Virbasius^{1,2}, Ling Lin^{1,2}, Lihua J. Zhu^{2,5}, Narendra Wajapeyee⁶ & Michael R. Green^{1,2}

The *TRIM37* (also known as *MUL*) gene is located in the 17q23 chromosomal region, which is amplified in up to ~40% of breast cancers¹. *TRIM37* contains a RING finger domain, a hallmark of E3 ubiquitin ligases², but its protein substrate(s) is unknown. Here we report that *TRIM37* mono-ubiquitinates histone H2A, a chromatin modification associated with transcriptional repression³. We find that in human breast cancer cell lines containing amplified 17q23, *TRIM37* is upregulated and, reciprocally, the major H2A ubiquitin ligase RNF2 (also known as RING1B)^{3,4} is downregulated. Genome-wide chromatin immunoprecipitation (ChIP)-chip experiments in 17q23-amplified breast cancer cells identified many genes, including multiple tumour suppressors, whose promoters were bound by *TRIM37* and enriched for ubiquitinated H2A. However, unlike RNF2, which is a subunit of polycomb repressive complex 1 (PRC1)³⁻⁵, we find that *TRIM37* associates with polycomb repressive complex 2 (PRC2). *TRIM37*, PRC2 and PRC1 are co-bound to specific target genes, resulting in their transcriptional silencing. RNA-interference-mediated knockdown of *TRIM37* results in loss of ubiquitinated H2A, dissociation of PRC1 and PRC2 from target promoters, and transcriptional reactivation of silenced genes. Knockdown of *TRIM37* in human breast

cancer cells containing amplified 17q23 substantially decreases tumour growth in mouse xenografts. Conversely, ectopic expression of *TRIM37* renders non-transformed cells tumorigenic. Collectively, our results reveal *TRIM37* as an oncogenic H2A ubiquitin ligase that is overexpressed in a subset of breast cancers and promotes transformation by facilitating silencing of tumour suppressors and other genes.

We previously identified *TRIM37* as a factor required for epigenetic silencing of the *Fas* tumour suppressor gene, and found that *TRIM37* was bound to the silenced *Fas* promoter in *Kras*-transformed NIH 3T3 cells⁶. Mono-ubiquitination of histone H2A at lysine 119 is associated with transcriptional repression³ and we considered the possibility that *TRIM37* was a histone H2A E3 ubiquitin ligase.

To test this idea, we first performed ChIP experiments to assess ubiquitinated H2A (H2Aub) levels on the epigenetically repressed *Fas* promoter. H2Aub was enriched at the silenced *Fas* promoter in *Kras*-transformed NIH 3T3 cells, and was lost after short hairpin RNA (shRNA)-mediated knockdown of *TRIM37* (Extended Data Fig. 1a–c). By contrast, H2Aub was retained after knockdown of RNF2, the major H2A ubiquitin ligase involved in gene regulation^{3,4}, or BMI1, a PRC1 component^{7,8} that stimulates RNF2 activity^{7,9}.

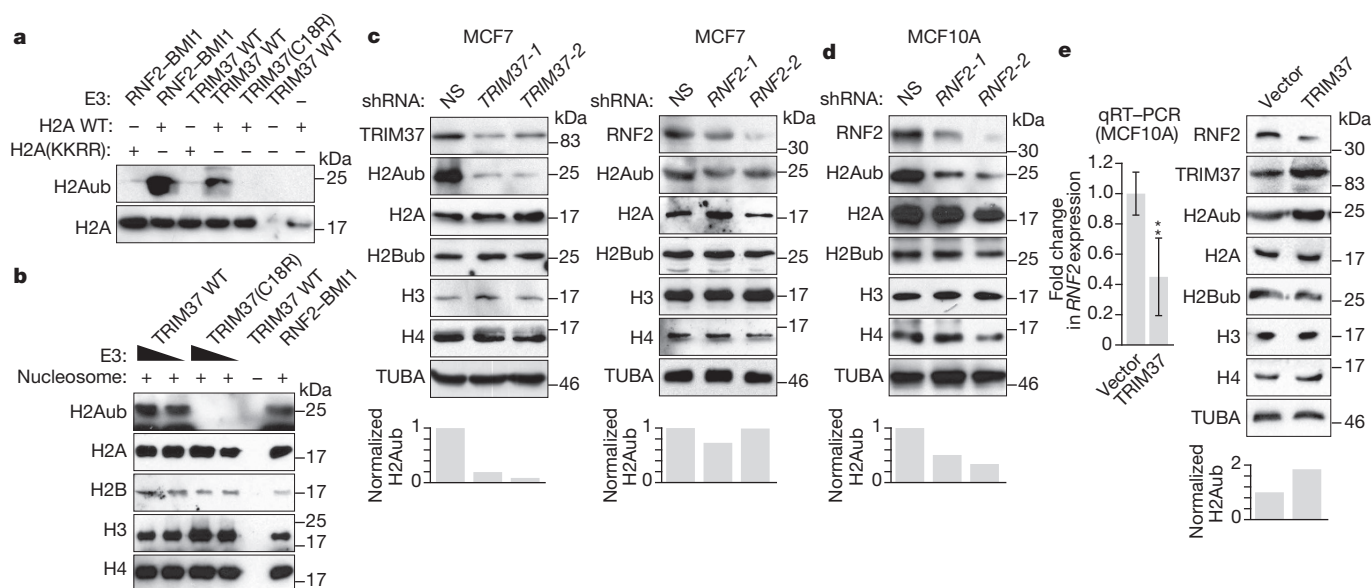


Figure 1 | *TRIM37* is a histone H2A ubiquitin ligase that is overexpressed in 17q23-amplified human breast cancer cell lines. **a, b**, *In vitro* ubiquitination assays with H2A wild type (WT) or H2A(KKRR) (a), or reconstituted nucleosomes (b). **c**, Top, immunoblots in MCF7 cells expressing a non-silencing (NS), *TRIM37* or *RNF2* shRNA. Bottom, quantification of H2Aub relative to α -tubulin (TUBA); H2Aub in NS cells was set to 1. **d**, Immunoblots

in MCF10A cells expressing an NS or *RNF2* shRNA. **e**, qRT-PCR (left) and immunoblots (right) in MCF10A cells expressing *TRIM37* or vector. *RNF2* expression and H2Aub levels were normalized to that obtained with vector. Error bars indicate standard error of the mean (s.e.m.); $n = 3$ technical replicates of a representative experiment (out of three experiments). * $P < 0.05$; ** $P < 0.01$.

¹Howard Hughes Medical Institute, University of Massachusetts Medical School, Worcester, Massachusetts 01605, USA. ²Programs in Gene Function and Expression and Molecular Medicine, University of Massachusetts Medical School, Worcester, Massachusetts 01605, USA. ³CEA/DSV/iRCM/LEFG, Genopole G2, and Université Paris Diderot, 91057 Evry, France. ⁴Boehringer Ingelheim Pharmaceuticals, Inc., Ridgefield, Connecticut 06877, USA. ⁵Program in Bioinformatics and Integrative Biology, University of Massachusetts Medical School, Worcester, Massachusetts 01605, USA. ⁶Department of Pathology, Yale University School of Medicine, New Haven, Connecticut 06520, USA.

We next assessed whether TRIM37 could mono-ubiquitinate H2A at lysine 119. Purified recombinant TRIM37 or, as a positive control, the RNF2–BMI1 complex, was incubated in the presence of an E1 ubiquitin-activating enzyme, an E2 ubiquitin-conjugating enzyme, ATP and haemagglutinin (HA)-tagged ubiquitin. Like RNF2–BMI1, TRIM37 could mono-ubiquitinate purified H2A, but not an H2A derivative mutated at the K118/K119 ubiquitination site (H2A(KKRR))¹⁰ or H2B (Fig. 1a and Extended Data Fig. 1d). By contrast, a TRIM37 derivative bearing a point mutation in a conserved cysteine residue in the RING finger motif (C18R), which interferes with catalytic activity², failed to promote H2A mono-ubiquitination (Fig. 1a). Furthermore, wild-type TRIM37, but not TRIM37(C18R), could mono-ubiquitinate H2A in an assembled nucleosome (Fig. 1b).

We next analysed the relationship between expression of TRIM37 and RNF2 in several human breast cancer cell lines containing amplified 17q23 (MCF7, BT474 and MDA-MB-361)¹¹. As controls, we analysed in parallel a non-transformed human breast epithelial cell line that lacked 17q23 amplification (MCF10A) and immortalized human mammary epithelial cells (HMECs). Breast cancer cell lines containing amplified 17q23 expressed substantially higher levels of TRIM37, but lower levels of RNF2, compared with MCF10A cells and HMECs (Extended Data Fig. 1e–g).

Consistent with these expression results, knockdown of TRIM37 in MCF7, BT474 or MDA-MD-361 cells markedly decreased total H2Aub levels (Fig. 1c, left, and Extended Data Fig. 1h–j). By contrast, knockdown of RNF2 (Extended Data Fig. 1k) in MCF7 cells had only a modest effect on H2Aub levels (Fig. 1c, right), but substantially reduced H2Aub levels in MCF10A cells (Fig. 1d). Moreover, knockdown of TRIM37 did not have a major effect on H2Aub levels in breast cancer cell lines lacking 17q23 amplification (Extended Data Fig. 1l, m).

The expression results shown in Extended Data Fig. 1e, f suggested a reciprocal relationship between TRIM37 and RNF2 expression levels. Consistent with this possibility, ectopic expression of TRIM37 in MCF10A cells (Extended Data Fig. 1n) resulted in downregulation of RNF2 (Fig. 1e).

To identify TRIM37 target genes in MCF7 cells, we performed global ChIP–chip analysis and identified 9,412 genes that were bound by TRIM37, 7,638 of which were also enriched for H2Aub (Fig. 2a, Extended Data Fig. 2a and Supplementary Table 1). Knockdown of TRIM37 resulted in loss or reduction of H2Aub in ~75% of these genes (Fig. 2b, Extended Data Fig. 2a, b and Supplementary Table 1). Searches of cancer-gene databases revealed that 469 TRIM37 target genes are putative tumour suppressors (Supplementary Table 1). Notably, there was a statistically significant enrichment of putative tumour suppressors among the genes bound by TRIM37 ($P = 1.99 \times 10^{-5}$).

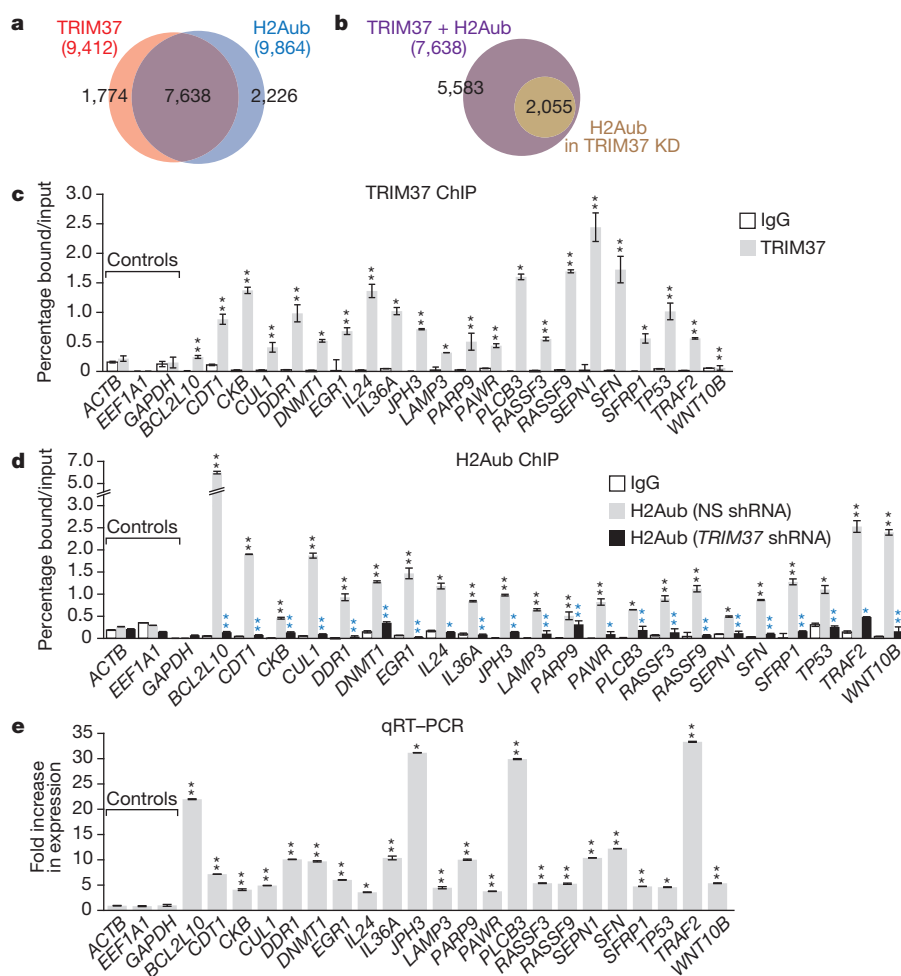


Figure 2 | Identification of TRIM37 target genes. **a, b**, Venn diagrams showing overlap between TRIM37-bound and H2Aub-enriched genes in parental MCF7 cells (**a**) or after TRIM37 knockdown (KD; **b**). See also Supplementary Table 1. **c**, TRIM37 ChIP in MCF7 cells. *ACTB*, *EEF1A1* and *GAPDH* are negative controls. Error bars indicate s.e.m.; $n = 3$ technical replicates of a representative experiment (out of three experiments). **d**, H2Aub ChIP in MCF7 cells expressing an NS or *TRIM37* shRNA. IgG from cells expressing an NS shRNA is shown. Error bars indicate standard deviation

(s.d.); $n = 3$ technical replicates of a representative experiment (out of three experiments). Black asterisks indicate significance of H2Aub enrichment compared with IgG; blue asterisks indicate significant differences in H2Aub enrichment in cells expressing a *TRIM37* relative to an NS shRNA. **e**, qRT–PCR monitoring target gene expression in TRIM37 knockdown MCF7 cells. Error bars indicate s.e.m.; $n = 3$ technical replicates of a representative experiment (out of three experiments). * $P < 0.05$; ** $P < 0.01$.

To validate the ChIP-chip results, we analysed a representative set of 22 putative tumour suppressor and other genes in directed ChIP experiments using promoter-specific primer pairs. For all 22 genes analysed, TRIM37 and H2Aub were significantly enriched at the promoter (Fig. 2c, d and Extended Data Fig. 3a, b). For the majority of these genes, enrichment of H2Aub substantially decreased after knockdown of TRIM37 but not RNF2 (Fig. 2d and Extended Data Fig. 3b, c). Finally, knockdown of TRIM37 but not RNF2 substantially increased expression of all TRIM37 target genes analysed (Fig. 2e and Extended Data Fig. 3d, e). Knockdown of TRIM37 in BT474 cells also resulted in increased expression of a subset of TRIM37 target genes analysed (Extended Data Fig. 3f–h).

Previous studies have shown that RNF2 functions through association with PRC1 (refs 3–5). We next performed a series of experiments to determine whether TRIM37 also functioned through PRCs. We first asked whether TRIM37 was physically associated with PRC1 or PRC2. To test this idea, MCF7 cell nuclear extract was fractionated by sucrose gradient sedimentation and individual fractions were analysed by immunoblotting for TRIM37 and PRC subunits. The results shown in Fig. 3a demonstrate that TRIM37 co-sedimented with PRC2 subunits EZH2 and SUZ12 (refs 8, 12, 13). Physical interactions between TRIM37 and PRC2 subunits could be demonstrated by co-immunoprecipitation (Fig. 3b and Extended Data Fig. 4a–c), liquid chromatography tandem mass spectroscopy (Extended Data Fig. 4d, e and Supplementary Table 2), an *in vitro* pull-down assay (Extended Data Fig. 4f), and the ability of a

GAL4–TRIM37 fusion protein to recruit PRC2 subunits to GAL4-binding sites (Extended Data Fig. 4g).

Global ChIP-chip analysis identified 3,384 genes that were co-bound by TRIM37 and EZH2 (Fig. 3c, Extended Data Fig. 2a and Supplementary Table 3). In addition, 3,560 genes were bound by TRIM37 and enriched for histone H3 lysine 27 trimethylation (H3K27me3) (Fig. 3d, Extended Data Fig. 2a, c and Supplementary Table 4). Knockdown of TRIM37 resulted in loss or reduction of H3K27me3 in ~65% of these genes (Fig. 3e, Extended Data Fig. 2a, d and Supplementary Table 4). Several studies have reported global correlations between PRC1/PRC2 occupancy and CpG islands^{14–18}. We found no statistically significant difference between the percentage of promoters co-bound by TRIM37 and EZH2 or bound by EZH2 alone that contain a CpG island (Extended Data Fig. 2e).

To validate the ChIP-chip results, we analysed a representative set of TRIM37 target genes for binding of EZH2 and BMI1 by directed ChIP assays. All gene promoters analysed were enriched for BMI1 and EZH2, which was diminished after TRIM37 knockdown (Fig. 3f and Extended Data Fig. 5a–c). These gene promoters were also enriched for H3K27me3, which was reduced after TRIM37 knockdown (Fig. 3g and Extended Data Fig. 5d). As expected, knockdown of BMI1 or EZH2 resulted in increased expression of these genes (Fig. 3h and Extended Data Fig. 5e, f).

Our results raised the possibility that in breast cancers containing amplified 17q23, TRIM37 is overexpressed and contributes to transformation by silencing tumour suppressor genes. To investigate the relationship

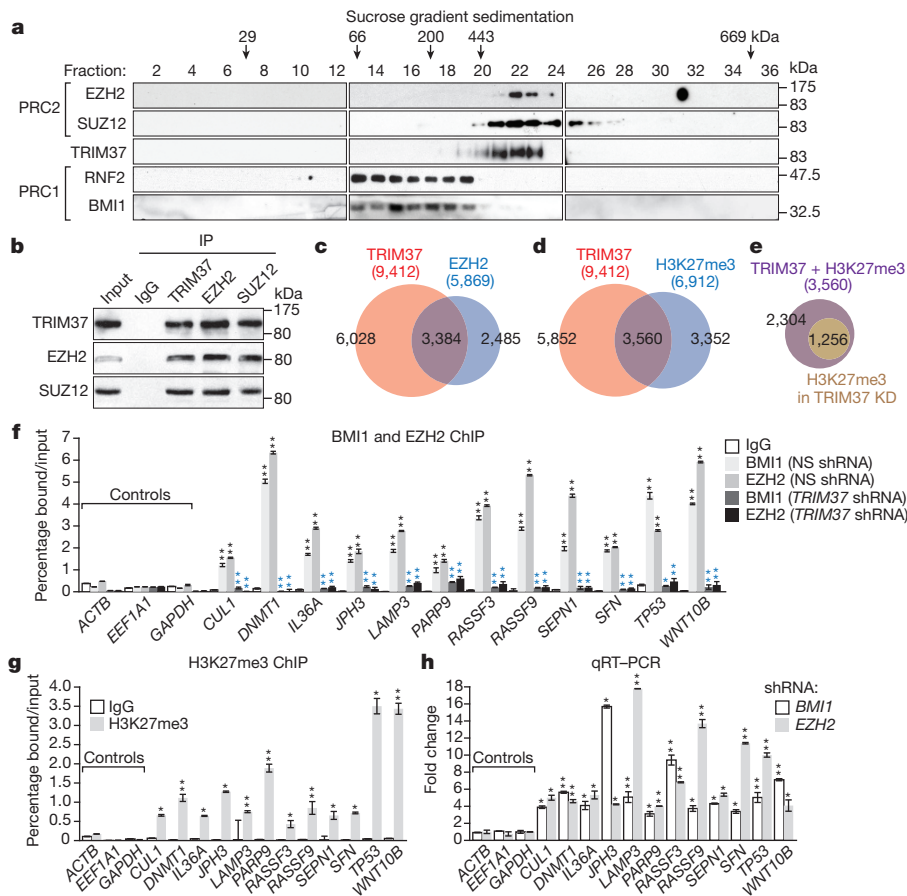


Figure 3 | Interaction and co-occupancy of TRIM37 and PRC2.

a, Immunoblots on sucrose gradient fractions. **b**, Sucrose gradient fractions 20–22 immunoprecipitated (IP) with a TRIM37, EZH2 or SUZ12 antibody, or an IgG control, were analysed by immunoblotting. **c–e**, Venn diagrams showing overlap between TRIM37- and EZH2-bound genes (**c**) and TRIM37-bound and H3K27me3-enriched genes (**d**) in parental MCF7 cells, or after knockdown of TRIM37 (**e**). See also Supplementary Tables 3 and 4. **f**, BMI1 and EZH2 ChIP in MCF7 cells expressing an NS or TRIM37 shRNA.

Error bars indicate s.d.; $n = 3$ technical replicates of a representative experiment (out of three experiments). **g**, H3K27me3 ChIP in MCF7 cells. Error bars indicate s.d.; $n = 3$ technical replicates of a representative experiment (out of three experiments). **h**, qRT-PCR monitoring TRIM37 target gene expression in BMI1- or EZH2-knockdown MCF7 cells. Error bars indicate s.e.m.; $n = 3$ technical replicates of a representative experiment (out of three experiments). * $P < 0.05$; ** $P < 0.01$.

between TRIM37 levels and the expression of TRIM37 target genes, we analysed a published comprehensive data set of 466 human breast cancer samples¹⁹. Of the 9,412 TRIM37 target genes we identified, there was a statistically significant correlation between increased TRIM37 levels and decreased expression of 2,794 genes (Supplementary Table 5). The heat map shown in Fig. 4a illustrates the results for 60 TRIM37 target genes in a subset of breast cancer samples in which TRIM37 is either under- or overexpressed (Extended Data Fig. 6).

To confirm that elevated TRIM37 levels were responsible for decreased TRIM37 target gene expression, we analysed expression of representative

TRIM37 target genes in MCF10A cells ectopically expressing TRIM37. Expression of all TRIM37 target genes analysed was significantly lower in cells ectopically expressing TRIM37 compared with empty vector (Fig. 4b).

To investigate directly the potential oncogenic activity of TRIM37, we knocked down TRIM37 in MCF7 cells and measured the effect on tumorigenicity in mouse xenografts. Knockdown of TRIM37 markedly reduced tumour growth (Fig. 4c) without affecting proliferation of cultured MCF7 cells (Fig. 4d and Extended Data Fig. 7a). Knockdown of TRIM37 also reduced tumour formation in xenografts derived from BT474 and FC-IBC02 breast cancer cells (Extended Data Fig. 7b, c).

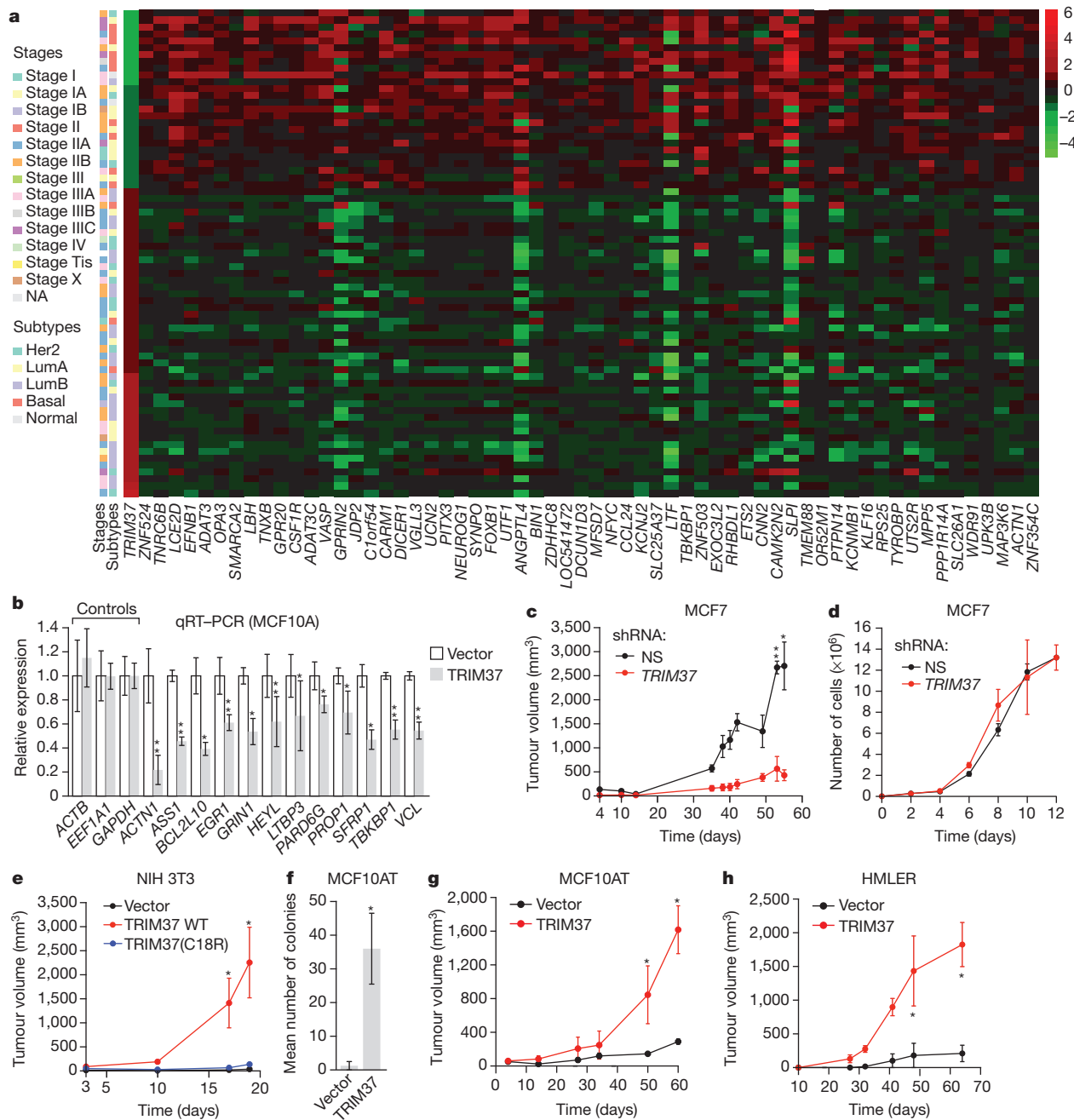


Figure 4 | TRIM37 is an oncogene. **a**, Heat map showing expression of TRIM37 and target genes in human breast cancer samples. See also Supplementary Table 5. **b**, qRT-PCR monitoring TRIM37 target gene expression in MCF10A cells expressing TRIM37 or vector. Error bars indicate s.e.m.; $n = 3$ technical replicates of a representative experiment (out of three experiments). **c**, Tumour formation in mice injected with MCF7 cells expressing an NS or TRIM37 shRNA. Error bars indicate s.e.m.; $n = 3$ mice per group. **d**, Proliferation of MCF7 cells expressing an NS or TRIM37 shRNA. Error bars indicate s.d.; $n = 3$

technical replicates of a representative experiment (out of three experiments). **e**, Tumour formation in mice injected with NIH 3T3 cells expressing vector, TRIM37 wild type (WT) or TRIM37(C18R). Error bars indicate s.e.m.; $n = 3$ mice per group. **f**, Soft agar assay with MCF10AT cells expressing vector or TRIM37. Error bars indicate s.e.m.; $n = 3$ technical replicates of a representative experiment (out of three experiments). **g**, **h**, Tumour formation in mice injected with MCF10AT (**g**) or HMLER (**h**) cells expressing vector or TRIM37. Error bars indicate s.e.m.; $n = 3$ mice per group. * $P < 0.05$; ** $P < 0.01$.

Conversely, ectopic expression of wild-type TRIM37 (Extended Data Fig. 7d), but not TRIM37(C18R), transformed NIH 3T3 cells, enabling tumour formation in mice (Fig. 4e). Moreover, ectopic expression of TRIM37 (Extended Data Fig. 7e) also transformed MCF10AT cells, a pre-malignant MCF10A derivative stably expressing activated *HRAS*^{S20}, enabling growth in soft agar (Fig. 4f) and tumour formation in mice (Fig. 4g). Furthermore, knockdown of a subset of TRIM37 target genes with predicted tumour suppressor activity also transformed MCF10AT cells (Extended Data Fig. 7f–h). By contrast, TRIM37 could not transform parental MCF10A cells (Extended Data Fig. 7i, j), indicating that TRIM37 can cooperate with RAS to transform human breast epithelial cells. Ectopic expression of TRIM37 also transformed HMLER and BPLER cells, immortalized human breast epithelial cell lines containing activated *HRAS*^{S21} (Fig. 4h and Extended Data Fig. 7k). Notably, the RAS pathway is activated in ~50% of breast cancers²².

We have identified a new H2A ubiquitin ligase and shown how it functions in conjunction with PRCs to silence target genes. In the canonical silencing pathway, PRC2 first interacts with the promoter, followed by EZH2-catalysed H3K27 trimethylation, which is recognized by PRC1, followed by RNF2-catalysed H2A ubiquitination^{8,13}. In cells containing high TRIM37 levels, TRIM37 associates with PRC2 and the TRIM37–PRC2 complex targets specific promoters. The promoter-bound PRC2–TRIM37 complex then carries out both H3K27 trimethylation and H2A mono-ubiquitination (see Extended Data Fig. 8a). Our results show that in the absence of PRC2, TRIM37 can catalyse H2A mono-ubiquitination (Fig. 1a, b) and bind to DNA (Fig. 3c). However, it remains possible that association with PRC2 could modulate, positively or negatively, the DNA-binding or H2A mono-ubiquitination activity of TRIM37. TRIM37 is also required for PRC1 occupancy, which presumably is mediated by PRC2 as in the canonical pathway. Although PRC1 does not direct H2A ubiquitination, it is still required for silencing, consistent with previous studies showing that PRC1 mediates other repressive activities, such as chromatin compaction^{23,24}.

TRIM37 alters the specificity of PRC2 and thus when TRIM37 is overexpressed there are extensive changes in gene expression that include the silencing of multiple tumour suppressor genes. Our results are consistent with previous studies showing that altered PRC2 activity, resulting, for example, from overexpression of EZH2, leads to malignancy^{25,26}. In support of our cell culture results, we found a correlation between increased TRIM37 levels and decreased expression of TRIM37 target genes in human breast cancer samples (Fig. 4a and Supplementary Table 5). Interestingly, there is also a statistically significant correlation between high levels of TRIM37 and decreased survival in patients with oestrogen-receptor-positive breast cancer (Extended Data Fig. 8b). Collectively, our results reveal TRIM37 as a new H2A ubiquitin ligase that is overexpressed and promotes transformation in a subset of breast cancers.

Online Content Methods, along with any additional Extended Data display items and Source Data, are available in the online version of the paper; references unique to these sections appear only in the online paper.

Received 28 October 2013; accepted 9 October 2014.

Published online 24 November 2014.

1. Sinclair, C. S., Rowley, M., Naderi, A. & Couch, F. J. The 17q23 amplicon and breast cancer. *Breast Cancer Res. Treat.* **78**, 313–322 (2003).
2. Budhidarmo, R., Nakatani, Y. & Day, C. L. RINGs hold the key to ubiquitin transfer. *Trends Biochem. Sci.* **37**, 58–65 (2012).
3. Weake, V. M. & Workman, J. L. Histone ubiquitination: triggering gene activity. *Mol. Cell* **29**, 653–663 (2008).
4. Wang, H. *et al.* Role of histone H2A ubiquitination in Polycomb silencing. *Nature* **431**, 873–878 (2004).

5. de Napoles, M. *et al.* Polycomb group proteins Ring1A/B link ubiquitylation of histone H2A to heritable gene silencing and X inactivation. *Dev. Cell* **7**, 663–676 (2004).
6. Gazin, C., Wajapeyee, N., Gobeil, S., Virbasius, C. M. & Green, M. R. An elaborate pathway required for Ras-mediated epigenetic silencing. *Nature* **449**, 1073–1077 (2007).
7. Cao, R., Tsukada, Y. & Zhang, Y. Role of Bmi-1 and Ring1A in H2A ubiquitylation and Hox gene silencing. *Mol. Cell* **20**, 845–854 (2005).
8. Lanzuolo, C. & Orlando, V. Memories from the polycomb group proteins. *Annu. Rev. Genet.* **46**, 561–589 (2012).
9. Buchwald, G. *et al.* Structure and E3-ligase activity of the Ring–Ring complex of polycomb proteins Bmi1 and Ring1b. *EMBO J.* **25**, 2465–2474 (2006).
10. Richly, H. *et al.* Transcriptional activation of polycomb-repressed genes by ZRF1. *Nature* **468**, 1124–1128 (2010).
11. Monni, O. *et al.* Comprehensive copy number and gene expression profiling of the 17q23 amplicon in human breast cancer. *Proc. Natl Acad. Sci. USA* **98**, 5711–5716 (2001).
12. Kirmizis, A. *et al.* Silencing of human polycomb target genes is associated with methylation of histone H3 Lys 27. *Genes Dev.* **18**, 1592–1605 (2004).
13. Margueron, R. & Reinberg, D. The Polycomb complex PRC2 and its mark in life. *Nature* **469**, 343–349 (2011).
14. Ku, M. *et al.* Genomewide analysis of PRC1 and PRC2 occupancy identifies two classes of bivalent domains. *PLoS Genet.* **4**, e1000242 (2008).
15. Mohn, F. *et al.* Lineage-specific polycomb targets and *de novo* DNA methylation define restriction and potential of neuronal progenitors. *Mol. Cell* **30**, 755–766 (2008).
16. Velichutina, I. *et al.* EZH2-mediated epigenetic silencing in germinal center B cells contributes to proliferation and lymphomagenesis. *Blood* **116**, 5247–5255 (2010).
17. Orlando, D. A., Guenther, M. G., Frampton, G. M. & Young, R. A. CpG island structure and trithorax/polycomb chromatin domains in human cells. *Genomics* **100**, 320–326 (2012).
18. Riising, E. M. *et al.* Gene silencing triggers polycomb repressive complex 2 recruitment to CpG islands genome wide. *Mol. Cell* **55**, 347–360 (2014).
19. Cancer Genome Atlas Network. Comprehensive molecular portraits of human breast tumours. *Nature* **490**, 61–70 (2012).
20. Miller, F. R. *et al.* Xenograft model of progressive human proliferative breast disease. *J. Natl. Cancer Inst.* **85**, 1725–1732 (1993).
21. Ince, T. A. *et al.* Transformation of different human breast epithelial cell types leads to distinct tumor phenotypes. *Cancer Cell* **12**, 160–170 (2007).
22. von Lintig, F. C. *et al.* Ras activation in human breast cancer. *Breast Cancer Res. Treat.* **62**, 51–62 (2000).
23. Grau, D. J. *et al.* Compaction of chromatin by diverse Polycomb group proteins requires localized regions of high charge. *Genes Dev.* **25**, 2210–2221 (2011).
24. Eskeland, R. *et al.* Ring1B compacts chromatin structure and represses gene expression independent of histone ubiquitination. *Mol. Cell* **38**, 452–464 (2010).
25. Chang, C. J. & Hung, M. C. The role of EZH2 in tumour progression. *Br. J. Cancer* **106**, 243–247 (2012).
26. Deb, G., Thakur, V. S. & Gupta, S. Multifaceted role of EZH2 in breast and prostate tumorigenesis: epigenetics and beyond. *Epigenetics* **8**, 464–476 (2013).

Supplementary Information is available in the online version of the paper.

Acknowledgements We thank C. Peterson for providing *Xenopus* nucleosomes; R. Weinberg and M. Cristofanilli for providing cell lines; A. Virbasius and the University of Massachusetts Medical School (UMMS) RNAi Core Facility for providing shRNAs; P. Spatrick at the UMMS Genomics Core Facility; the UMMS Proteomics and Mass Spectroscopy Facility for mass spectrometry analysis; and S. Deibler for providing editorial assistance. N.W. is a Sidney Kimmel Scholar for Cancer Research and is supported by young investigator awards from the National Lung Cancer Partnership/United Against Lung Cancer, Melanoma Research Alliance and International Association for the Study of Lung Cancer. This work was also supported by grants from CEA-DSV, ATIGE Genopole and Centre National de la Recherche Scientifique (CNRS) to C.G., and from the National Institutes of Health (R01GM033977) to M.R.G. M.R.G. is an investigator of the Howard Hughes Medical Institute.

Author Contributions C.G. made the initial observation that TRIM37 has an H2A mono-ubiquitination activity. S.B., C.G., J.S.T. and M.R.G. designed the experiments. S.B., L.C., X.Z., L.L. and N.W. performed the research. C.-M.V. provided critical reagents. J.O. and L.J.Z. performed biostatistical analysis for ChIP-chip experiments and database mining. S.B. and M.R.G. analysed and interpreted the data and wrote the paper. All authors reviewed the paper and provided comments.

Author Information The ChIP-chip data have been deposited in the Gene Expression Omnibus under accession number GSE48196. Reprints and permissions information is available at www.nature.com/reprints. The authors declare no competing financial interests. Readers are welcome to comment on the online version of the paper. Correspondence and requests for materials should be addressed to M.R.G. (michael.green@umassmed.edu).

METHODS

Cell lines and cell culture. K: Molv NIH 3T3 cells (ATCC# CRL-6361; referred to here as *Kras* NIH 3T3) were maintained in Dulbecco's modified eagle medium (DMEM) supplemented with 10% fetal calf serum (FCS) at 37 °C and 5% CO₂. HMECs (Life Technologies) were cultured in HuMec Ready Media (Life Technologies). MCF10A (ATCC) and MCF10AT²⁷ cells were maintained in DMEM/F12 supplemented with 5% horse serum (Invitrogen), EGF (Peprotech), hydrocortisone (Sigma), cholera toxin (Sigma), insulin (GIBCO) and penicillin/streptomycin (Life Technologies). MCF7 cells (National Cancer Institute) were maintained in DMEM supplemented with 1 × nonessential amino acids (NEAA) and 10% fetal bovine serum (FBS). BT474 cells (ATCC) were maintained in ATCC HybriCare Media supplemented with 10% FBS. MDA-MB-361 and MDA-MB-231 cells (ATCC) were cultured in ATCC-formulated Leibovitz's L-15 medium supplemented with 20% FBS. T47D cells (National Cancer Institute (NCI)) were maintained in RPMI medium supplemented with 10% FBS. Hs578T cells (NCI) were maintained in DMEM medium supplemented with 0.01 mg ml⁻¹ bovine insulin and 10% FBS. BPLER and HMLER cells²¹ (provided by R. Weinberg, Whitehead Institute, Massachusetts Institute of Technology) were maintained in WIT (Stemgent) and mammary epithelial cell growth medium (Lonza), respectively. FC-IBC02 cells²⁸ (provided by M. Cristofanilli, Thomas Jefferson University) were maintained in Ham's F12 Nutrient Mixture (Life Technologies) with 10% FBS and 0.5% insulin (Gibco) with 100 µg l⁻¹ hydrocortisone (Sigma) and antibiotic-antimycotic (Gibco). Cells cultured at the same time were pooled together and then seeded after counting in a 6-well or 10-cm dish. Dishes/wells were then subjected, in a random order, to treatment with a control or test shRNA/vector.

RNA interference. For stable shRNA knockdowns, cells were seeded in a six-well plate to 50% confluency and subsequently transduced with 400 µl lentiviral particles expressing shRNAs (obtained from Open Biosystems/Thermo Scientific through the UMMS RNAi Core Facility, listed in Extended Data Table 1) in a total volume of 2 ml of appropriate media supplemented with 6 µg ml⁻¹ polybrene. Media was replaced after overnight incubation to remove the polybrene and viral particles and cells were subjected to puromycin selection (2 µg ml⁻¹) for 3 days.

In vitro ubiquitination assays. To produce purified recombinant TRIM37, the TRIM37 open reading frame was PCR amplified from a cDNA clone (Invitrogen) using high fidelity Pfu polymerase, and cloned into a derivative of pEF6/V-5HisB (Invitrogen), resulting in the addition of a protein-C epitope (MAEDQVDPRLID GKFEFT) at the N terminus of TRIM37. The C18R mutation was introduced by overlap extension PCR using primers listed in Extended Data Table 2. All constructs were verified by sequencing.

In vitro ubiquitination reactions were set up containing purified TRIM37 or TRIM37(C18R) (500 ng to 2 µg), a combination of BMI1 (500 ng; Abcam) and RNF2 (500 ng; Origene) mixed together, or BRCA1 (500 ng; Abcam) plus H2A or H2B (5X; Boston Biochemicals), 10 nM UBE1 (E1; Boston Biochemicals), 10 nM UBCH5B (E2; Boston Biochemicals), and 10 nM HA-ubiquitin aldehyde (Boston Biochemicals) in 10 µl of reaction buffer (50 mM Tris-Cl, pH 7.9, 5 mM MgCl₂, 2 mM NaF, 100 mM dithiothreitol (DTT) and 2 mM ATP). Reactions were incubated at 32 °C for 90 min. For the nucleosomal assay, *in vitro* ubiquitination reactions were set up similarly but contained *Xenopus* oocyte-derived nucleosomes; recombinant histone particles were expressed and purified as described previously²⁹ and reconstituted using a standard salt step dialysis method³⁰. To generate the H2A(KKRR) mutant¹⁰, a pET-based plasmid expressing H2A (provided by C. Peterson, University of Massachusetts Medical School) was used as a template in a PCR-based site-directed mutagenesis with primer extension reaction using primers listed in Extended Data Table 2. Proteins were resolved by 15% SDS-PAGE and subjected to immunoblotting with H2Aub(K119) (Cell Signaling Technology #8240, clone D27C4), H2A (Cell Signaling Technology #2578), H2Bub (EMD Millipore 05-1312, clone 56), H2B (Abcam ab18977), H3 (Cell Signaling Technology #9715) or H4 (Cell Signaling Technology #2592) antibodies.

qRT-PCR. Total RNA was isolated and reverse transcribed using Superscript II Reverse Transcriptase (Invitrogen). Quantitative real-time PCR was performed as described previously⁶ using primers listed in Extended Data Table 2. Gene expression was normalized to *GAPDH*. Controls lacking reverse transcriptase were carried out in parallel to rule out the possibility of DNA contamination. Each sample was analysed three independent times and the results from one representative experiment, with technical triplicates, are shown.

Immunoblotting. Nuclear lysates were prepared as previously described³¹. Nuclear extracts were separated on either 8%, 10% or 20% SDS-PAGE gels. Blots were probed with primary antibodies (H2Aub(K119), Cell Signaling Technology; H2A, Cell Signaling Technology; H2Bub, EMD Millipore; H2B, Cell Signaling Technology #12364, clone D2H6; H, Cell Signaling Technology; H4, Cell Signaling Technology; HA, Cell Signaling Technology #2367, clone 6E2; TRIM37, Abcam ab95997, or custom made by 21st Century Biochemicals against a synthetic peptide corresponding to amino acids 444–460 of the human protein followed by affinity purification;

RNF2, Abcam ab28629; and α -tubulin, created in house) overnight at 4 °C, washed five times in TBS plus 0.1% Tween (TBST) and then incubated with the appropriate HRP-conjugated secondary antibody for 1 h at room temperature. Membranes were washed five times in TBST and visualized on autoradiography film after incubating with ECL reagent (Supersignal West Pico or Supersignal West Femto; Thermo Scientific). Immunoblots were quantified using ImageJ software v.1.47 (National Institutes of Health).

TRIM37 overexpression. A TRIM37 complementary DNA clone (Origene Technologies) was subcloned into the vector p3X-Flag-Myc-CMV-26 (Sigma) using NotI and XbaI sites, and verified by full-length sequencing. The TRIM37 expression vector was transfected into cells using Effectene reagent (Qiagen) and stable clones were selected. Overexpression of TRIM37 was confirmed by immunoblotting using TRIM37 (21st Century) and anti-Flag (Sigma M2) antibodies.

ChIP-chip and directed ChIP. For ChIP-chip analysis, chromatin was sonicated and immunoprecipitation was carried out as previously described³¹ using a TRIM37 (Abcam), H2Aub (Cell Signaling Technology), EZH2 (Cell Signaling Technology #5246, clone D2C9), or H3K27me3 (Cell Signaling Technology #9733, clone C36B11) antibody. Samples were prepared and hybridized to a GeneChip Human Promoter 1.0R Array (Affymetrix) according to the manufacturer's specifications, and arrays were scanned using a GeneChip Scanner 3000 7G (Affymetrix). Each ChIP-chip experiment was performed in duplicate. ChIP-chip data were analysed using Bioconductor package Starr^{32,33} for data read-in, normalizing and peak calling. Quantile normalization was applied to normalize probe intensity before peak calling with default settings except that fragment length (sonication fragment length) was set to 500, minrun (minimum number of probes in a bound region) was set to 2, method (multiple test adjustment method) was set to BH (Benjamini & Hochberg)³⁴, and α (false discovery rate cut-off) was set to 0.1. ChIP-chip results were annotated by an R (v.3.1.0)/Bioconductor (v.2.14)/ChIPpeakAnno(v.2.12.1) package³⁵. Density plots were plotted by the distance of peaks to the annotated transcription start site. Venn diagrams were drawn by an R (v.3.1.0)/Vennable (v.3.0) package. Gene ontology analysis was done by the R/Bioconductor package goProfiles³⁶. For the statistical analysis on the global decrease in H3K27me3 and H2A-ub following TRIM37 knockdown in MCF7 cells, the Wilcoxon signed-rank test was performed in R³⁷. A summary table showing the overlap of proteins and epigenetic marks, along with the *P* values for each overlap, is shown in Supplementary Table 6. CpG island overlap analysis was performed as previously described¹⁷ except that CpG island annotation was downloaded from the UCSC Genome Browser (<https://www.genome.ucsc.edu>). A CpG gene list was generated for CpG islands located within 1 kb upstream of the transcription start site. The percentage of promoters bound by EZH2 alone or co-bound by TRIM37 and EZH2 and which also contain a CpG island was calculated by the intersection of the CpG gene list and the EZH2 or EZH2/TRIM37 target gene list, respectively. The ChIP-chip data have been deposited in NCBI's Gene Expression Omnibus³⁸ and are accessible through accession number GSE48196.

Directed ChIP assays were performed essentially as described previously⁶ using cell extracts prepared 7 days after retroviral transduction and puromycin selection, and antibodies against BMI1 (Abcam ab14389, clone 1.T.21), EZH2 (Cell Signaling Technology), H3K27me3 (Cell Signaling Technology), H2Aub (Cell Signaling Technology) and TRIM37 (Abcam) or, as a negative control, IgG. The sequences of primers used for amplifying ChIP products are listed in Extended Data Table 2. On the basis of the probe sequence used in the Affymetrix array, for each gene a 400–600 bp region was tested for enrichment of TRIM37 using at least three primer pairs. The primer pair with the consistently highest enrichment in three different experiments was chosen for subsequent enrichment analysis of BMI1, H2Aub, H3K27me3 and EZH2. Each ChIP experiment was carried out three independent times and the results from one representative experiment, with technical triplicates, are shown.

Identification of putative tumour suppressors. Candidate TRIM37 target genes were systematically queried against three databases: DNA Tumour Suppressor and Oncogene Database (DTSOD; available at <http://embryology.med.unsw.edu.au>), TSGene database (TSGene; <http://bioinfo.mc.vanderbilt.edu/TSGene/>), and Tumour Associated Gene (TAG; <http://www.binfo.ncku.edu.tw/TAG/GeneDoc.php>). Genes listed in the TSGene database or listed as "tumour suppressor genes" in the DTSOD or TAG database were considered putative tumour suppressor genes. Statistical enrichment of putative tumour suppressor genes among TRIM37 target genes was calculated by a hypergeometric test.

Sucrose gradient fractionation. Sucrose gradient sedimentation analysis was performed as described³⁹. Briefly, 10–40% gradients were formed by layering 500 µl NEB1 buffer containing 10%, 20%, 30% or 40% sucrose in a 11 × 34 mm centrifuge tube (Beckman) and allowed to equilibrate at room temperature for 2 h. Gradients were chilled, loaded with 500 µg MCF7 nuclear extract (adjusted to a volume of 150 µl) or 150 µl molecular weight markers (Sigma MW-GF-1000), and centrifuged in a Beckman TLS-55 rotor at 214,000g for 14 h. Thirty-six fractions of 45 µl were collected. For the markers, 20 µl of each fraction was electrophoresed and Coomassie

stained. For the gradient fractions, 20 µl of fractions were analysed by immunoblotting using EZH2 (Cell Signaling Technology), SUZ12 (Abcam ab12073), TRIM37 (Abcam), RNF2 (Abcam ab101273) and BMI1 (Bethyl Laboratories, A301-694A). **Co-immunoprecipitation.** MCF7 nuclear extract (~1,000 µg) was incubated with a TRIM37 (Abcam), EZH2 (Cell Signaling Technology) or SUZ12 (Abcam) antibody at 4 °C for 24 h in the presence or absence of ethidium bromide (100 µg ml⁻¹). For immunoprecipitations from fractionated nuclear lysate, fractions 20–22 (which were enriched for TRIM37, EZH2 and SUZ12) were pooled and diluted 15-fold. Immune complexes were captured on rabbit or mouse TrueBlot IP beads (eBioScience), washed three times in NEB1 buffer, and eluted by boiling for 10 min in 2× SDS sample buffer. Immunoprecipitations from MCF7 cells ectopically expressing Flag-tagged TRIM37 were performed similarly, except that anti-Flag magnetic beads (Sigma) were used to capture the immune complexes. Immunoprecipitated proteins were analysed by immunoblotting as described earlier. Input lanes represent 10–25% of extract loaded in the immunoprecipitation lanes.

Liquid chromatography tandem mass spectrometry. Large-scale immunoprecipitation was carried out as previously described⁴⁰ by incubating 80 mg MCF7 nuclear extract with 50 µg of anti-TRIM37 antibody (Abcam) at 4 °C for 5 h. Immune complexes were captured on IgG Dynabeads (Life Technologies) by additional incubation at 4 °C for 2 h. The beads were then washed with NETN (20 mM Tris-HCl (pH 8.0), 0.1 M NaCl, 1 mM EDTA, 0.5% NP-40) three times and re-suspended in Laemmli buffer. Proteins were separated on a short 10% SDS-PAGE. A 2 cm gel slice with all the proteins was submitted for mass spectrometry at the University of Massachusetts Medical School Proteomics and Mass Spectrometry Facility.

For in-gel digestion, gel slices were placed in 1.5 ml Eppendorf tubes with 1 ml of water for 30 min and then replaced with 100 µl of 250 mM ammonium bicarbonate. For reduction, 20 µl of 45 mM DTT was added and the samples were incubated at 50 °C for 30 min. The alkylation was carried out by addition of 20 µl of a 100 mM iodoacetamide solution for 30 min. The gel slices were washed twice with water and then treated with 50:50 50 mM ammonium bicarbonate:acetonitrile for 1 h. The solution was then removed and 200 µl of acetonitrile was added. Dried gel slices were rehydrated in 50 µl of 2 ng µl⁻¹ trypsin (Sigma) in 0.01% ProteaseMAX Surfactant (Promega):50 mM ammonium bicarbonate at 37 °C for 21 h. Additional dehydration was carried out with 100 µl of 80:20 acetonitrile:1% formic acid. Dried samples were resuspended in 25 µl of 5% acetonitrile in 0.1% trifluoroacetic acid.

Samples were injected onto a custom packed 2 cm × 100 µm C₁₈ Magic 5 µm particle trap column. Labelled peptides were then eluted and sprayed from a custom packed emitter (75 µm × 25 cm C₁₈ Magic 3 µm particle) with a linear gradient from 95% solvent A (0.1% formic acid in water) to 35% solvent B (0.1% formic acid in acetonitrile) in 90 min at a flow rate of 300 nl per minute on a Waters Nano Acquity UPLC system. Data-dependent acquisitions were performed on a Q Exactive mass spectrometer (Thermo Scientific). Raw data files were processed with Proteome Discoverer (v.1.3) before searching with Mascot Server (v.2.4) against the Human Index of the SwissProt database. Search parameters used were fully tryptic with two missed cleavages, parent mass tolerances of 10 p.p.m. and fragment mass tolerances of 0.05 Da. A fixed modification of carbamidomethyl cysteine and variable modifications of acetyl (protein N-terminus), pyro glutamic for N-terminal glutamine, oxidation of methionine was considered. Search results were loaded into the Scaffold Viewer (Proteome Software), which provided total spectra scores and interaction probabilities.

GST pull-down assay. The *TRIM37* cDNA (Origene Technologies) was cloned into the vector pGEX4T-1 (Life Technologies) using EcoRI and NotI sites and the construct was verified by full-length sequencing. Supernatant from bacteria expressing GST-*TRIM37* was incubated with glutathione agarose beads (GE Healthcare) at 4 °C for 3–4 h. Beads were washed three times with PBS and 0.5% Triton X-100 before using in pull-down assays. PRC2 subunits (EZH2 (Origene Technologies), SUZ12 (Origene Technologies), AEBP2 (Open Biosystems), EED (Open Biosystems) and RBAP48 (Open Biosystems)) were *in vitro* translated using the TnT T7 Quick Coupled Transcription/Translation System (Promega) according to the manufacturer's specifications. GST-*TRIM37* beads (3 µg) were incubated with *in vitro* translated protein (added to 1/10 volume of the reaction mixture) in Buffer A (50 mM Tris-HCl pH 7.9, 0.5 mM EDTA, 1 mM DTT, 0.2 mM PMSF, 10% glycerol, 150 mM KCl and 0.05% NP40) at 4 °C for 2 h. After incubation, beads were washed twice with wash buffer (50 mM Tris-HCl pH 7.9, 0.5 mM EDTA, 1 mM DTT, 0.2 mM PMSF, 10% glycerol, 300 mM KCl and 0.05% NP40). The interaction was detected by immunoblot using a biotin antibody (Abcam #53494).

GAL4-*TRIM37* recruitment assay. The *TRIM37* cDNA was cloned into the plasmid pCMX-Gal4 (Addgene), which contains amino acids 1–147 of GAL4, using KpnI and NheI sites. *TRIM37* deletions were generated using PCR-based site-directed deletion with primer extension using primers listed in Extended Data Table 2. All constructs were verified by full-length sequencing. 293T cells were co-transfected with the GAL4-*TRIM37* plasmid and G5E1bcat-pSP72 (ref. 41) (containing five

GAL4-binding sites) or E1bcat-pSP72 (ref. 42) (negative control). CHIP assays were carried out as described earlier.

Breast cancer biostatistical analysis. Gene expression and CpG methylation data from breast cancer samples ($n = 466$) were obtained from The Cancer Genome Atlas (TCGA) Data Portal (https://tcga-data.nci.nih.gov/docs/publications/brca_2012/)¹⁹. The mRNA data were converted to relative mRNA expression levels by subtracting each gene's median level computed over 22 tumour-adjacent normal controls from its level observed in each patient sample. A subset of samples was then selected for further analysis to include those with upregulated *TRIM37* ($n = 45$ with *TRIM37* value ≥ 1) and downregulated *TRIM37* ($n = 26$ with *TRIM37* value ≤ -1). Pearson correlation analysis was performed to identify *TRIM37* target genes (identified in the ChIP-chip experiment) whose downregulation significantly correlated with increased *TRIM37* expression ($P < 0.01$). Statistical analysis and plotting were done with R (v.3.1.0), a system for statistical computation and graphics³⁷. The top 60 genes with negative correlation to *TRIM37* were extracted for heat map plots using an R (v.3.1.0)/pheatmap (v.0.7.7) package. Cancer subtypes were extracted from sample list information of gene expression data (level 3, PAM50). Cancer stages were extracted from TCGA clinical information.

TRIM37/17q23 copy number data were also downloaded from https://tcga-data.nci.nih.gov/docs/publications/brca_2012/, section "SNP and Copy Number" Level 3 Data Archives. Data were visualized using R/Bioconductor package Gviz and analysed as described previously¹⁹. Briefly, thresholded gene level copy number values were calculated using GISTIC 2.0 and log₂ copy number values were thresholded as followed: values < -1 are set to -2 , values between -1 and -0.3 are set to -1 , values between -0.3 and 0.3 are set to 0 , values between 0.3 and 1 are set to 1 , and values > 1 are set to 2 . Tumours in which all gene level thresholded copy number changes equalled 0 were excluded from the analysis.

For correlation analysis between *TRIM37* and prognosis, Kaplan–Meier plotting and log-rank test were done at <http://kmpplot.com/analysis/index.php?p=service&cancer=breast>. Analysis was restricted to breast cancer patients with ER-positive subtypes. Patients were divided into two classes based on *TRIM37* expression: patients with higher than upper quartile *TRIM37* expression were considered to belong to the high-expressing *TRIM37* group ($n = 352$) and the other patients were considered to belong to the low-expressing *TRIM37* group ($n = 1,061$).

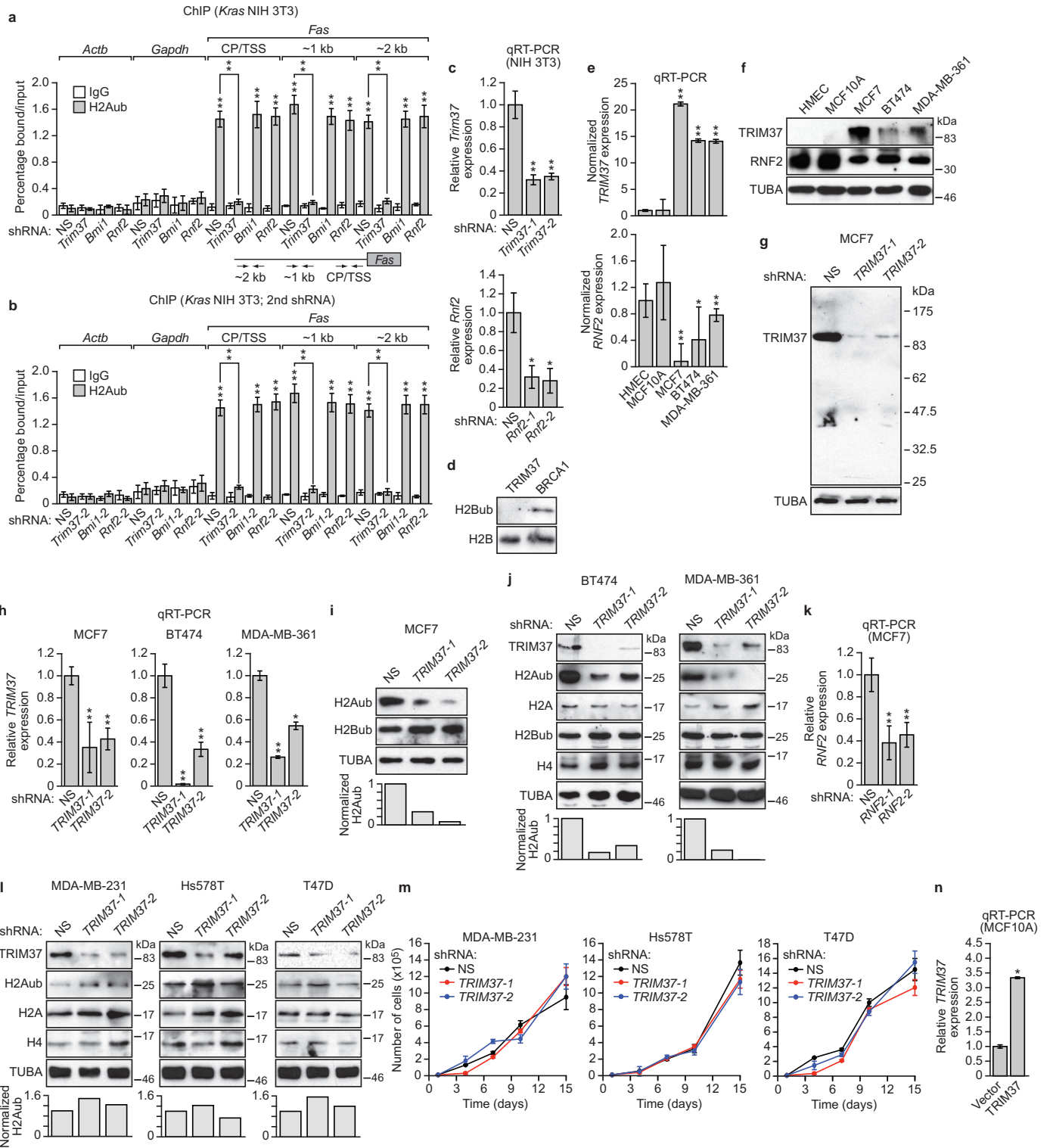
Animal experiments. All animal protocols were approved by the Institution Animal Care and Use Committee at UMMS (A-2016). Animal sample sizes were selected based on precedents established from previous publications and an understanding that at least $n = 5$ is generally required to achieve statistical significance. For mouse experiments involving shRNAs, the most efficacious shRNA of multiple shRNAs tested and validated in cell culture was used, a criterion that was established prospectively. Mice were randomly allocated to each group. No blinding was done as animal groups were identified by tagging and labelling the cages with the cells injected. Animals were excluded, according to pre-established criteria, if the tumour volume reached $>2,000$ mm³; if tumour size or location affected the mobility or general health of animal, the animal was euthanized and excluded from the experiment or the complete experiment was terminated.

MCF7 (1×10^6), BT474 (3×10^6) or FC-IBC02 (3×10^6) cells stably expressing a non-silencing (NS) or *TRIM37* shRNA were injected into the right thoracic mammary fat pad (MCF7) or flank (BT474 and FC-IBC02) of 6–8-week-old BALB/c nu/nu female mice ($n = 3$; Taconic Farms) to produce orthotopic primary tumours. Because MCF7, BT474 and FC-IBC02 cells are hormone dependent, a 60 day release tablet of 1.7 mg oestradiol (Innovative Research of America) was implemented under the skin of the neck of the mouse with a 11-gauge trocar. Primary tumour growth was evaluated by measurement with callipers. NIH 3T3 (5×10^6), MCF10AT (3×10^6), HMLER (3×10^6) or BPLER (3×10^6) cells expressing vector or *TRIM37* or *TRIM37*(C18R) were subcutaneously injected in the flank of the mice ($n = 3$) and the growth of the primary tumours was monitored as previously described⁶. MCF10AT (5×10^6) cells expressing an NS shRNA or shRNA targeting a tumour suppressor gene were subcutaneously injected in the flank of the mice ($n = 3$) and tumour growth was monitored. All mouse experiments were repeated at least twice (for a total of at least 6 mice per group).

Soft agar assay. MCF10AT cells (2.5×10^4) expressing vector or *TRIM37*, or MCF10AT cells expressing an NS shRNA or shRNA targeting a tumour suppressor gene, were re-suspended in 3 ml of top agar (MCF10AT media containing 0.3% Difco Noble agar (BD Biosciences)) warmed to 40 °C. The cell suspension was layered onto 3 ml of set bottom agar (MCF10AT media containing 0.7% Noble agar) in a 6-well plate. Two millilitres of medium was added on the top agar the next day and changed every other day. Visible colonies were scored after 4–5 weeks.

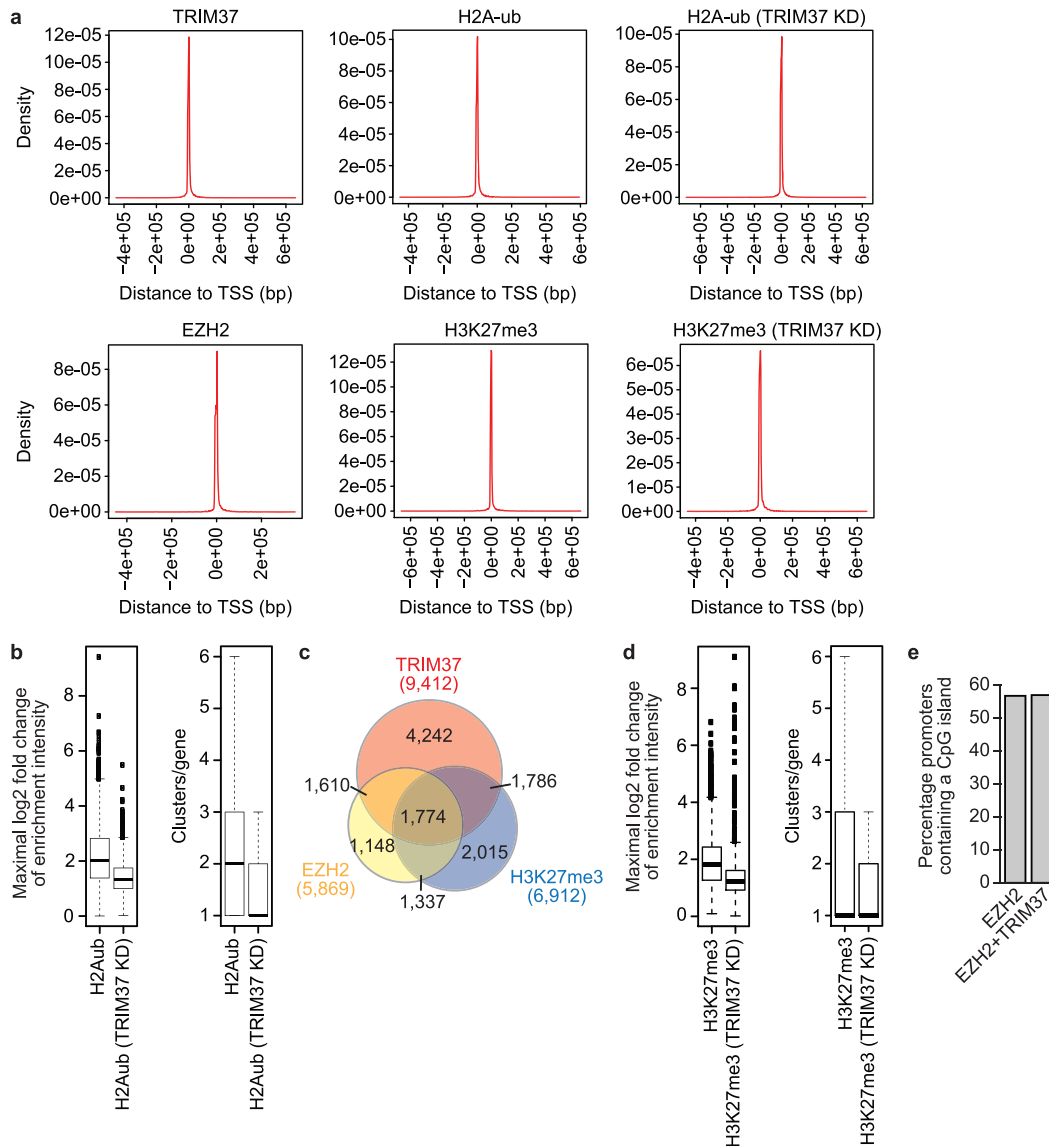
Statistics. To achieve statistical significance, all qRT-PCR and CHIP data were collected from experiments performed in technical triplicate; each experiment was repeated at least twice and statistically significant results were obtained in independent biological replicates. Differences between groups were assayed using a two-tailed student *t*-test using Microsoft Excel. In cases where the assumption of the

- t*-test was not valid, a non-parametric statistical method was used (for example, Wilcoxon signed-rank test). Significant differences were considered when $P < 0.05$; $*P \leq 0.05$ and $**P \leq 0.01$. Error bars indicate the standard deviation or standard error of the mean for the technical replicates, as indicated in figure legends.
27. Dawson, P. J., Wolman, S. R., Tait, L., Heppner, G. H. & Miller, F. R. MCF10AT: a model for the evolution of cancer from proliferative breast disease. *Am. J. Pathol.* **148**, 313–319 (1996).
 28. Fernandez, S. V. *et al.* Inflammatory breast cancer (IBC): clues for targeted therapies. *Breast Cancer Res. Treat.* **140**, 23–33 (2013).
 29. Luger, K., Rechsteiner, T. J. & Richmond, T. J. Expression and purification of recombinant histones and nucleosome reconstitution. *Methods Mol. Biol.* **119**, 1–16 (1999).
 30. Hansen, J. C., Ausio, J., Stanik, V. H. & van Holde, K. E. Homogeneous reconstituted oligonucleosomes, evidence for salt-dependent folding in the absence of histone H1. *Biochemistry* **28**, 9129–9136 (1989).
 31. Maston, G. A. *et al.* Non-canonical TAF complexes regulate active promoters in human embryonic stem cells. *eLife* **1**, e00068 (2012).
 32. Gentleman, R. C. *et al.* Bioconductor: open software development for computational biology and bioinformatics. *Genome Biol.* **5**, R80 (2004).
 33. Zacher, B., Kuan, P. F. & Tresch, A. Starr: Simple Tiling ARRay analysis of Affymetrix ChIP-chip data. *BMC Bioinformatics* **11**, 194 (2010).
 34. Benjamini, Y. & Hochberg, Y. Controlling the false discovery rate: a practical and powerful approach to multiple testing. *J. R. Statist. Soc. B* **57**, 289–300 (1995).
 35. Zhu, L. J. *et al.* ChIPpeakAnno: a Bioconductor package to annotate ChIP-seq and ChIP-chip data. *BMC Bioinformatics* **11**, 237 (2010).
 36. Salicrú, M., Ocana, J. & Sanchez-Pla, A. Comparison of lists of genes based on functional profiles. *BMC Bioinformatics* **12**, 401 (2011).
 37. Ihaka, R. & Gentleman, R. R. a language for data analysis and graphics. *J. Comput. Graph. Stat.* **5**, 299–314 (1996).
 38. Edgar, R., Domrachev, M. & Lash, A. E. Gene Expression Omnibus: NCBI gene expression and hybridization array data repository. *Nucleic Acids Res.* **30**, 207–210 (2002).
 39. Tanese, N. Small-scale density gradient sedimentation to separate and analyze multiprotein complexes. *Methods* **12**, 224–234 (1997).
 40. Wang, Y. *et al.* BASC, a super complex of BRCA1-associated proteins involved in the recognition and repair of aberrant DNA structures. *Genes Dev.* **14**, 927–939 (2000).
 41. Liu, F. & Green, M. R. A specific member of the ATF transcription factor family can mediate transcription activation by the adenovirus E1a protein. *Cell* **61**, 1217–1224 (1990).
 42. Lillie, J. W. & Green, M. R. Transcription activation by the adenovirus E1a protein. *Nature* **338**, 39–44 (1989).



Extended Data Figure 1 | Control experiments for Fig. 1. **a**, ChIP monitoring H2Aub enrichment on *Fas* in *Kras* NIH 3T3 cells expressing a non-silencing (NS) shRNA or a *Trim37*, *Rnf2* or *Bmi1* shRNA. Three regions of the *Fas* promoter were analysed: the core promoter/transcription start site (CP/TSS), and 1 and 2 kb upstream of the TSS. *Actb* and *Gapdh* are shown as negative controls. Error bars indicate s.e.m.; $n = 9$ (three biological replicates with three technical replicates per sample). **b**, H2Aub ChIP as described in **a** using a second *Trim37*, *Rnf2* or *Bmi1* shRNA unrelated to that used in **a**. **c**, qRT-PCR analysis monitoring knockdown efficiencies of *Trim37* and *Rnf2* shRNAs in NIH 3T3 cells. The results are given relative to expression after treatment with an NS shRNA, which was set to 1. For knockdown efficiencies of the *Bmi1* shRNAs see ref. 6. Error bars indicate s.e.m.; $n = 3$ technical replicates of a representative experiment (out of three experiments). **d**, *In vitro* ubiquitination assay. Purified H2B was incubated with E1 (UBE1), E2 (UBCH5B), E3 (*TRIM37* or *BRCA1*), ATP and HA-tagged ubiquitin. Blots were probed with antibodies against H2Bub or H2B. The results show that *TRIM37* does not ubiquitinate H2B. *BRCA1*, which is known to ubiquitinate H2B at K120 (refs 39, 40) was used as a positive control. **e**, **f**, qRT-PCR (**e**) and immunoblots (**f**) monitoring *TRIM37* and *RNF2* in various cell lines. Expression of *TRIM37* and *RNF2* was normalized to that obtained in HMECs, which was set to 1. Error bars indicate s.d.; $n = 3$ technical replicates of a representative experiment (out of three experiments). **g**, Immunoblot monitoring *TRIM37* levels in MCF7 cells expressing an NS or one of two unrelated *TRIM37* shRNAs. α -Tubulin (TUBA) was monitored as a loading control. The results indicate that the *TRIM37* antibody is highly specific. **h**, qRT-PCR analysis monitoring knockdown efficiencies of *TRIM37* shRNAs

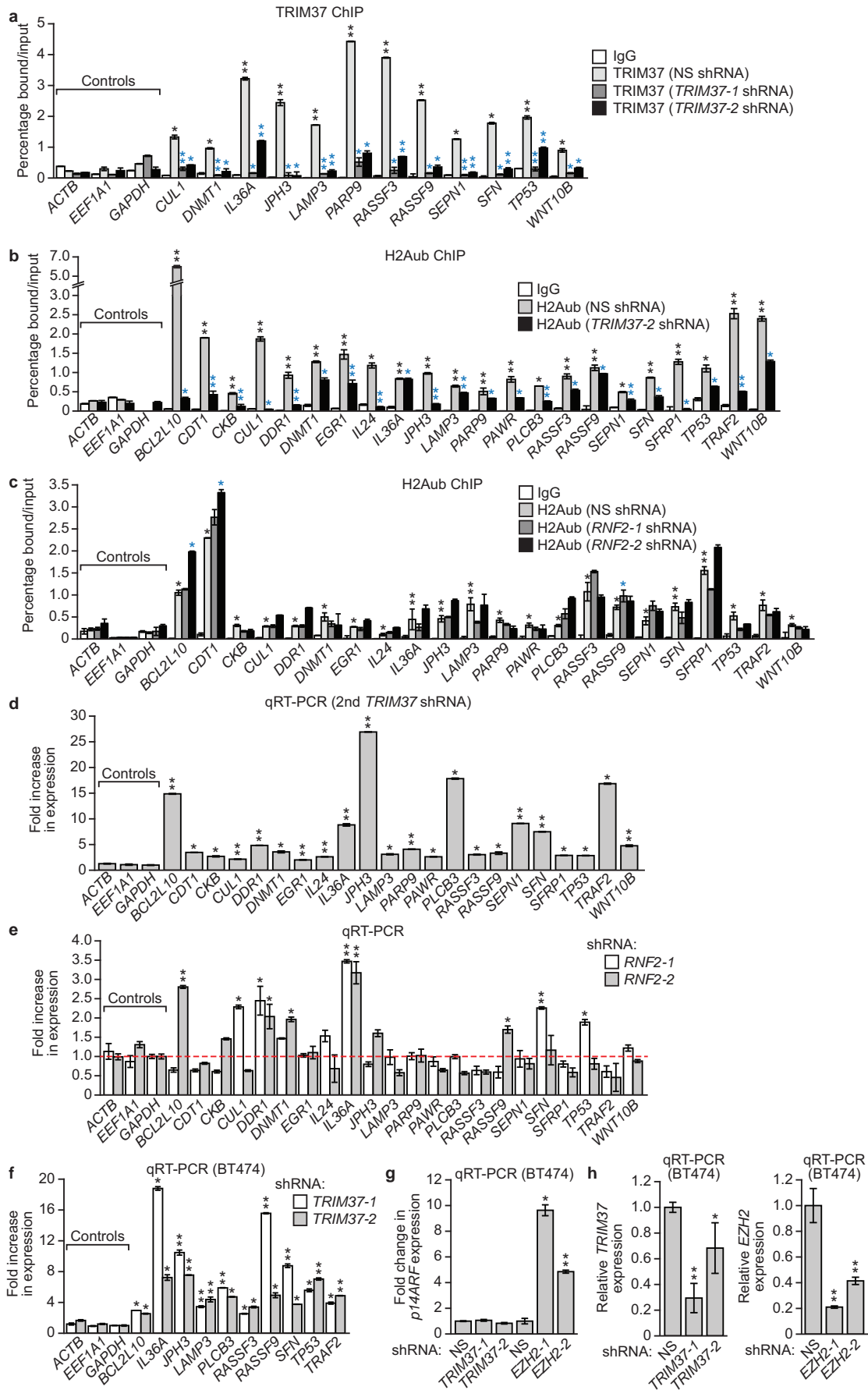
in MCF7, BT474 and MDA-MD-361 cells. Error bars indicate s.e.m.; $n = 3$ technical replicates of a representative experiment (out of three experiments). **i**, Top, immunoblots monitoring levels of H2Aub and H2Bub in MCF7 cells expressing an NS or one of two unrelated *TRIM37* shRNAs. Bottom, quantification of the H2Aub immunoblots relative to TUBA. The relative level of H2Aub in NS cells was set to 1. In this experiment, histones were acid extracted. **j**, Top, immunoblots monitoring *TRIM37*, H2Aub, H2A, H2Bub and H4 in BT474 and MDA-MB-361 cells expressing an NS or one of two unrelated *TRIM37* shRNAs. Bottom, H2Aub quantification, as described in **g**. **k**, qRT-PCR analysis monitoring knockdown efficiencies of *RNF2* shRNAs in MCF7 cells. Error bars indicate s.e.m.; $n = 3$ technical replicates of a representative experiment (out of three experiments). **l**, Top, immunoblots monitoring *TRIM37*, H2Aub, H2A and H4 in MDA-MB-231, Hs578T and T47D cells expressing an NS or one of two unrelated *TRIM37* shRNAs. Bottom, H2Aub quantification, as described in **g**. **m**, Proliferation of cultured MDA-MB-231, Hs578T and T47D cells expressing an NS or *TRIM37* shRNA. Error bars indicate s.d.; $n = 3$ technical replicates of a representative experiment (out of three experiments). The results show that knockdown of *TRIM37* has no effect on proliferation of breast cancer cell lines lacking 17q23 amplification. **n**, qRT-PCR analysis monitoring *TRIM37* expression in an MCF10A cell line ectopically expressing *TRIM37* or, as a control, empty vector. The results were normalized to *TRIM37* expression in MCF10A cells expressing empty vector, which was set to 1. Error bars indicate s.e.m.; $n = 3$ technical replicates of a representative experiment (out of three experiments). * $P < 0.05$, ** $P < 0.01$.



Extended Data Figure 2 | Extra details related to ChIP-chip analysis.

a, Histograms showing enrichment of TRIM37, H2Aub (in parental MCF7 cells or after TRIM37 knockdown (KD)), EZH2 and H3K27me3 (in parental MCF7 cells or after TRIM37 knockdown) as a function of distance to the nearest transcription start site (TSS). **b**, Left, box plot of maximal gene-level log₂ fold change of enrichment intensity comparing input for H2Aub in parental MCF7 cells and after TRIM37 knockdown. Right, box plot of number of enriched regions per gene for H2Aub in parental MCF7 cells or after TRIM37 knockdown. The results show that there was a significant difference in H2Aub enrichment at TRIM37 target genes after TRIM37 knockdown with respect to both enrichment intensity ($P < 1 \times 10^{-22}$) and number of enriched regions ($P = 2.787008 \times 10^{-222}$). A region with a fold change ≥ 2 and a false discovery rate < 0.1 was considered a differentially enriched site. **c**, Venn diagram showing overlap between TRIM37- and EZH2-bound genes and H3K27me3-enriched genes in MCF7 cells. **d**, Left, box plot of maximal gene-level log₂ fold

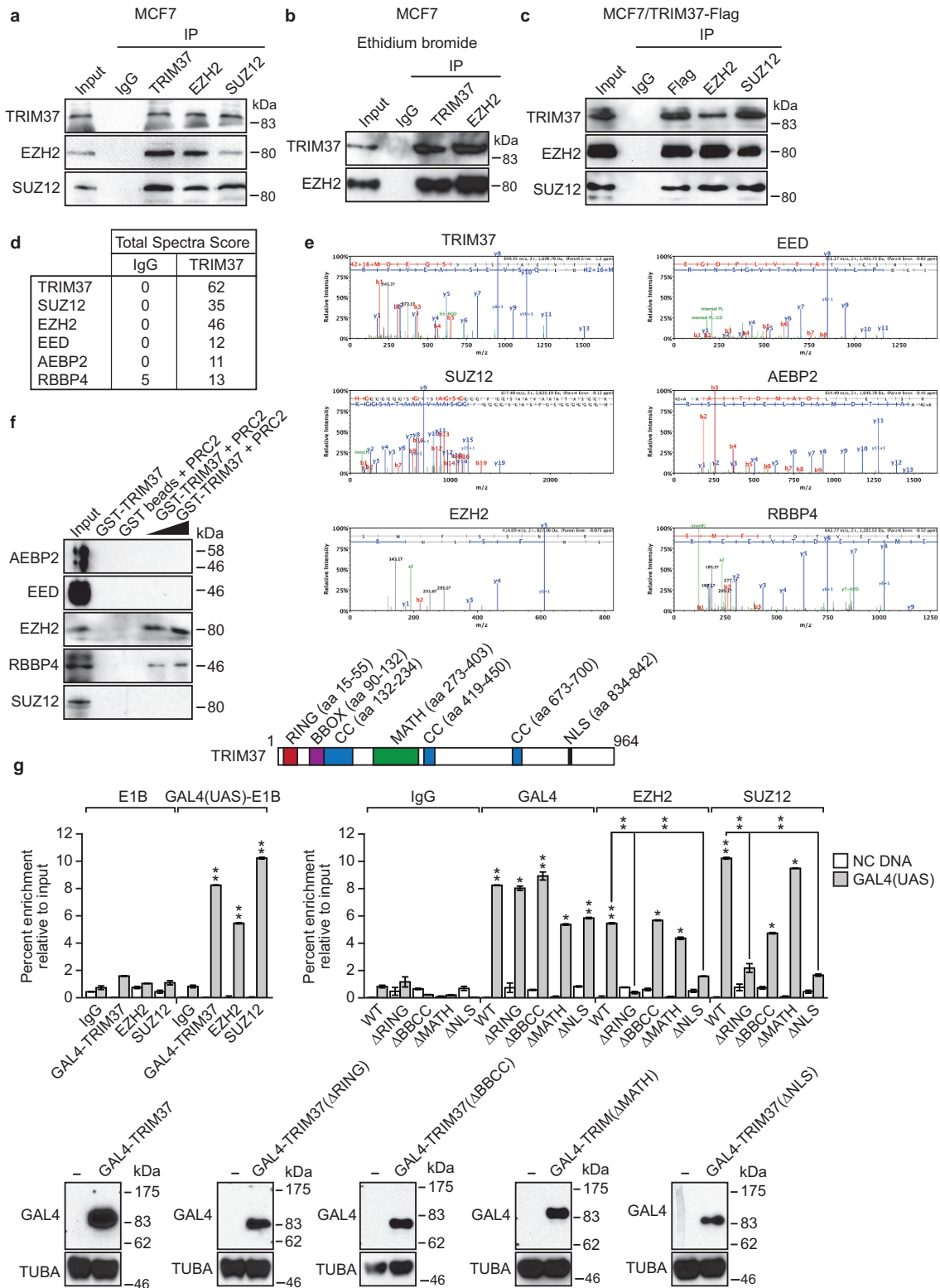
change of enrichment intensity comparing input for H3K27me3 in parental MCF7 cells or after TRIM37 knockdown. Right, box plot of number of enriched regions per gene for H3K27me3 in parental MCF7 cells or after TRIM37 knockdown. The results show that there was a significant difference in H3K27me3 enrichment at TRIM37 target genes after TRIM37 knockdown with respect to both enrichment intensity ($P = 5.872777 \times 10^{-109}$) and number of enriched regions ($P = 1.178392 \times 10^{-52}$). A region with a fold change ≥ 2 and a false discovery rate < 0.1 was considered a differentially enriched site. **e**, Percentage of promoters (defined as 1 kb upstream of the TSS) bound by EZH2 alone that contain a CpG island (3,332/5,869; 56.77%) or co-bound by EZH2 and TRIM37 that contain a CpG island (1,929/3,384; 57.00%). A two-sample test for equality of proportions with continuity correction showed that there was no statistically significant difference in CpG island content between the EZH2-bound and EZH2, TRIM37 co-bound promoters.



Extended Data Figure 3 | Control experiments for Fig. 2.

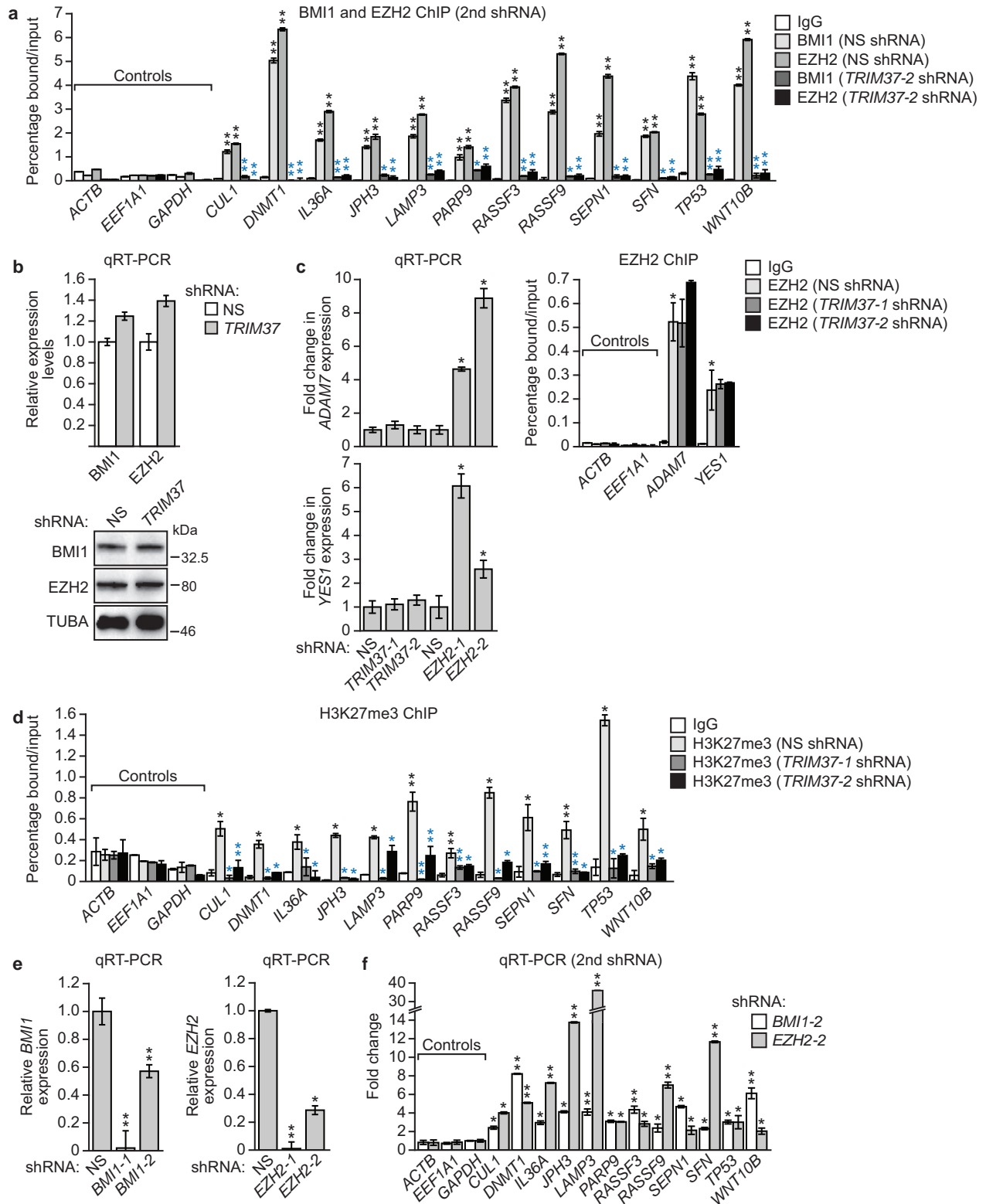
a, ChIP monitoring binding of TRIM37 at promoters of TRIM37 target genes in MCF7 cells expressing an NS or one of two unrelated *TRIM37* shRNAs. As a negative control, TRIM37 binding at three non-TRIM37 target genes, *ACTB*, *EEF1A1* and *GAPDH*, is shown. Black asterisks indicate significance of TRIM37 enrichment compared with the IgG control (from cells expressing an NS shRNA); blue asterisks indicate significant differences in TRIM37 enrichment in cells expressing a *TRIM37* shRNA relative to NS shRNA. Error bars indicate s.d.; $n = 3$ technical replicates of a representative experiment (out of three experiments). The results confirm that TRIM37 occupancy is reduced upon TRIM37 knockdown, demonstrating the specificity of the TRIM37 antibody in ChIP experiments. **b**, ChIP monitoring enrichment of H2Aub at promoters of TRIM37 target genes in MCF7 cells expressing a second *TRIM37* shRNA unrelated to that used in Fig. 2d. The IgG control and H2Aub signal in cells expressing an NS shRNA are the same as those shown in Fig. 2d. Error bars indicate s.d.; $n = 3$ technical replicates of a representative experiment (out of three experiments). **c**, ChIP monitoring enrichment of H2Aub at the promoters of TRIM37 target genes in MCF7 cells expressing an NS or one of two unrelated *RNF2* shRNAs. Error bars indicate s.d.; $n = 3$ technical replicates of a representative experiment (out of three experiments). **d**, qRT-PCR analysis

monitoring expression of TRIM37 target genes in MCF7 cells expressing a second *TRIM37* shRNA unrelated to that used in Fig. 2e. Expression of each gene was normalized to that obtained with an NS shRNA, which was set to 1. Error bars indicate s.e.m.; $n = 3$ technical replicates of a representative experiment (out of three experiments). **e**, qRT-PCR analysis monitoring expression of TRIM37 target genes after *RNF2* knockdown in MCF7 cells. Expression of each gene was normalized to that obtained with an NS shRNA, which was set to 1 (indicated by the dotted red line). Error bars indicate s.e.m.; $n = 3$ technical replicates of a representative experiment (out of three experiments). **f**, qRT-PCR analysis monitoring expression of TRIM37 target genes after TRIM37 knockdown in BT474 cells. Error bars indicate s.e.m.; $n = 3$ technical replicates of a representative experiment (out of three experiments). **g**, qRT-PCR analysis monitoring expression of *p14ARF* after knockdown of TRIM37 or *EZH2* in BT474 cells. Error bars indicate s.e.m.; $n = 3$ technical replicates of a representative experiment (out of three experiments). The results indicate that knockdown of *EZH2* but not TRIM37 de-represses *p14ARF* expression in BT474 cells. **h**, qRT-PCR analysis monitoring knockdown efficiencies of *TRIM37* (left) and *EZH2* (right) shRNAs in BT474 cells. Error bars indicate s.e.m.; $n = 3$ technical replicates of a representative experiment (out of three experiments). * $P < 0.05$, ** $P < 0.01$.



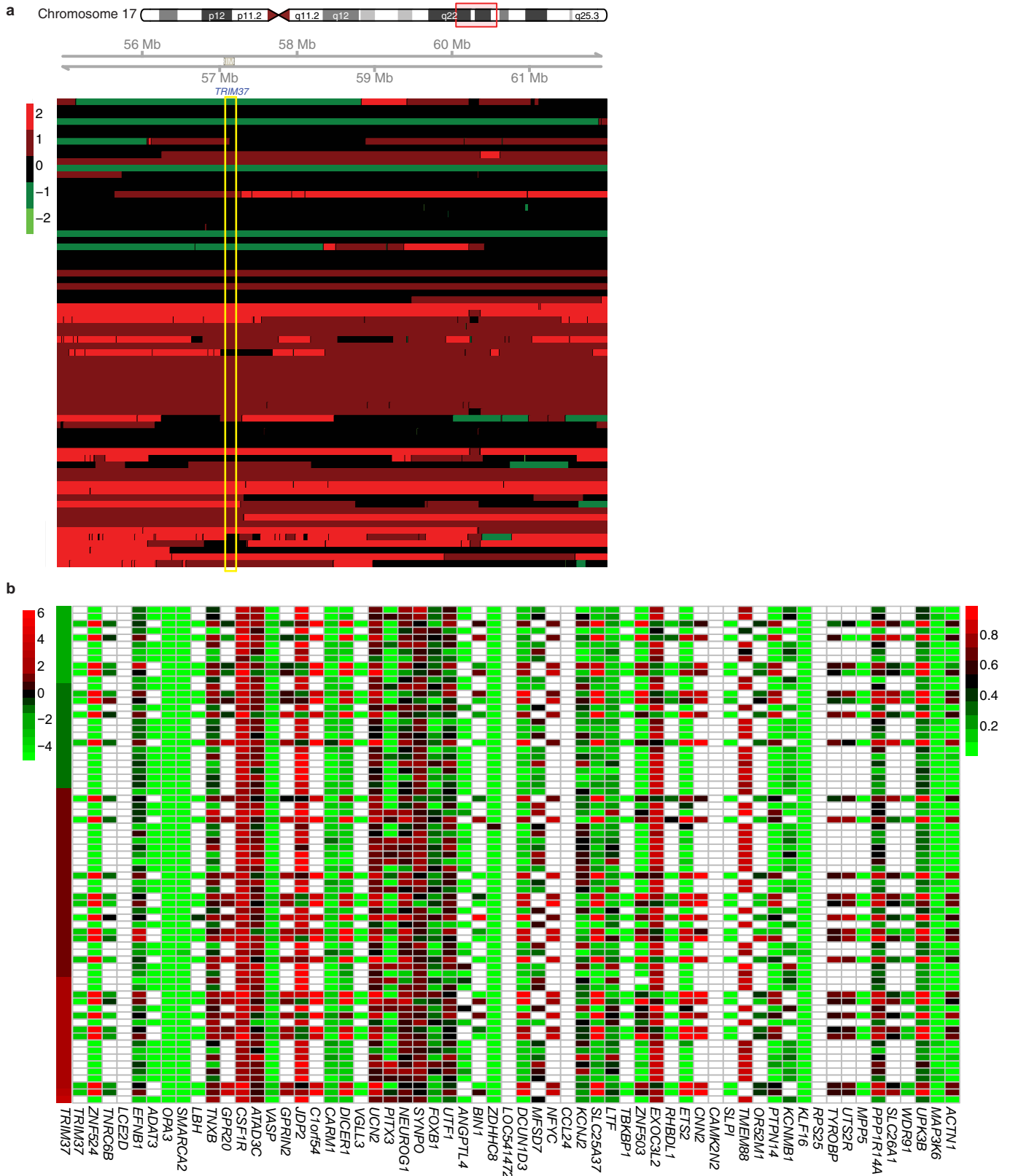
Extended Data Figure 4 | Additional experiments showing interaction between TRIM37 and PRC2 subunits. **a**, Co-immunoprecipitation analysis. MCF7 nuclear extracts were immunoprecipitated with a TRIM37, EZH2 or SUZ12 antibody, or an IgG control, and the immunoprecipitates were analysed for TRIM37, EZH2 or SUZ12 by immunoblotting. **b**, Co-immunoprecipitation analysis. MCF7 nuclear extracts were immunoprecipitated with a TRIM37 or EZH2 antibody, or an IgG control, in the presence of ethidium bromide, and the immunoprecipitates were analysed for TRIM37 or EZH2 by immunoblotting. The results show that interaction between TRIM37 and EZH2 occurs in the presence of ethidium bromide and is thus not mediated by DNA. **c**, Co-immunoprecipitation analysis. Nuclear extracts from MCF7 cells ectopically expressing Flag-TRIM37 were immunoprecipitated with anti-Flag magnetic beads, a EZH2 or SUZ12 antibody, or an IgG control, and the immunoprecipitates were analysed for TRIM37, EZH2 or SUZ12 by immunoblotting. **d**, Mass spectroscopy. Selected results from the liquid chromatography tandem mass spectroscopy analysis listing TRIM37 or PRC2 subunits, and their total spectra score in samples immunoprecipitated using either IgG or a TRIM37 antibody. The probability of interaction, derived from the Scaffold Viewer software, indicates a $\geq 95\%$ probability of interaction in all cases. See also Supplementary Table 2. **e**, Tandem mass spectra of representative peptides of proteins identified in the TRIM37 immunoprecipitate are shown with corresponding spectral counts for each protein shown in the table. **f**, *In vitro* interaction pull-down assay. Purified glutathione-S-transferase (GST)-TRIM37 was incubated with an *in vitro* translated biotinylated PRC2 subunit (indicated on left). GST-TRIM37 was purified using GST-agarose beads, and the presence of the PRC2 subunit

was analysed by immunoblotting with an anti-biotin antibody. The results indicate that TRIM37 interacts strongly with EZH2 and weakly with RBBP4, and does not detectably interact with AEBP2, EED or SUZ12. **g**, GAL4-TRIM37 fusion experiment. Top, schematic diagram of TRIM37 showing the location of the RING, BBOX, coiled coil (CC), MATH and nuclear localization sequence (NLS) motifs. Locations of the motifs were obtained from UniProtKB (http://www.uniprot.org/uniprot/O94972#section_attribute). The Δ BCC deletion comprises the BBOX and first CC motif (Δ aa 89–235). Middle, left, ChIP monitoring binding of GAL4-TRIM37, EZH2 or SUZ12 to the adenovirus *E1B* promoter containing (GAL4(UAS)-E1B) or lacking (E1B) GAL4-binding sites or to an irrelevant, negative control (NC) DNA region. The indicated GAL4-TRIM37 fusion protein was co-expressed with a plasmid containing or lacking five GAL4-binding sites upstream of the adenovirus *E1B* gene in 293T cells followed by ChIP analysis. Error bars indicate s.d.; $n = 3$ technical replicates of a representative experiment (out of three experiments). The results indicate that the GAL4-TRIM37 fusion protein was able to recruit both EZH2 and SUZ12 to the GAL4-binding sites. Middle, right, ChIP monitoring binding of EZH2 and SUZ12 in the presence of GAL4-TRIM37 deletion mutants. The GAL4-TRIM37 wild-type (WT) samples are the same as those shown in the left panel. The results indicate that the ability of GAL4-TRIM37 to recruit EZH2 and SUZ12 requires the TRIM37 RING domain and NLS (presumably for nuclear entry), but not the BBOX or MATH domains. Bottom, immunoblot analysis monitoring expression of GAL4-TRIM37 fusion proteins using a GAL4 antibody. α -Tubulin (TUBA) was monitored as a loading control.



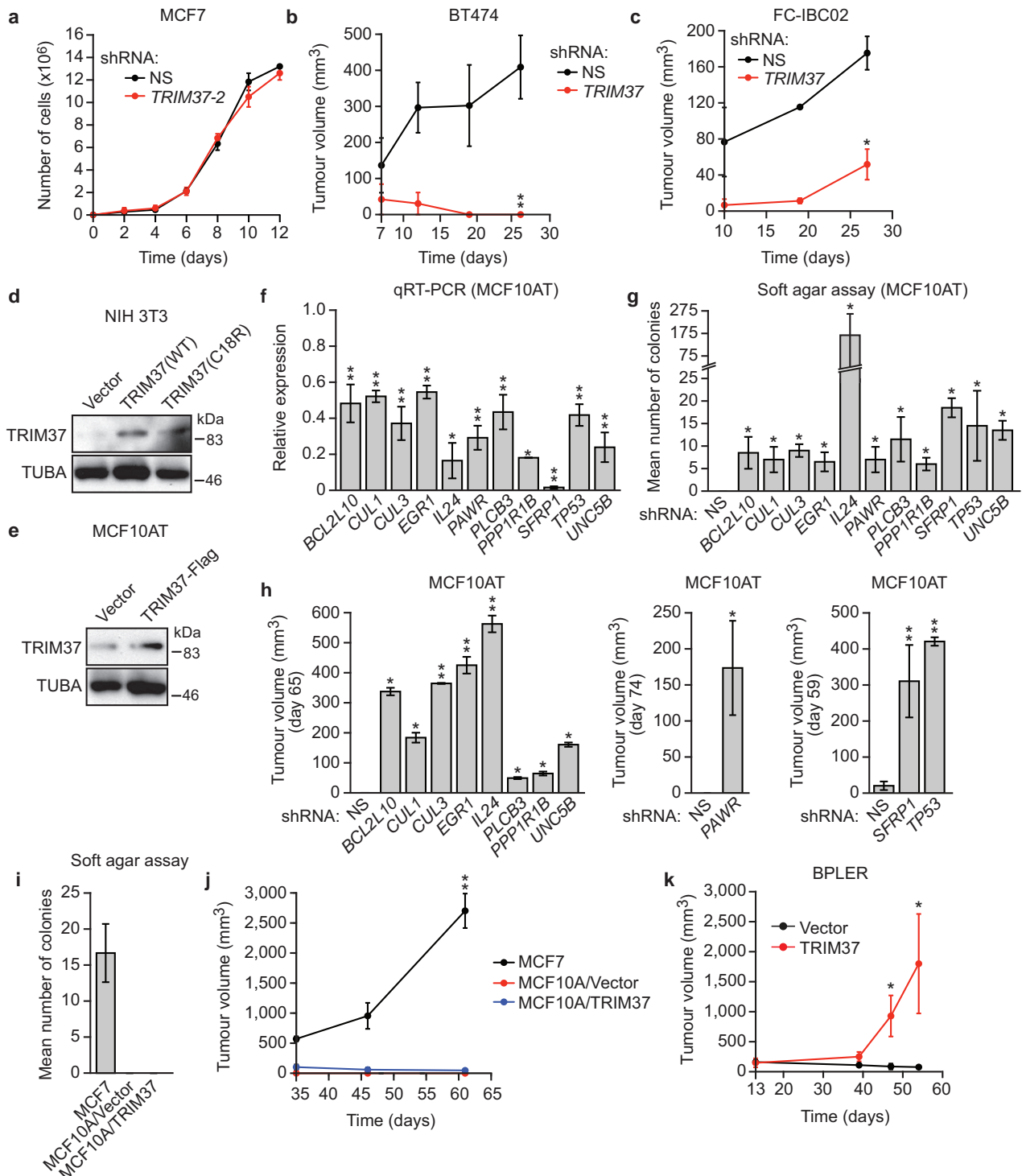
Extended Data Figure 5 | Confirmation of the results of Fig. 3f, h using second, unrelated shRNAs. **a**, ChIP monitoring binding of BMI1 and EZH2 to the promoters of TRIM37 target genes in MCF7 cells expressing an NS shRNA or a second TRIM37 shRNA unrelated to that used in Fig. 3f. The IgG control and BMI1 and EZH2 signal in cells expressing an NS shRNA are the same as those shown in Fig. 3f. Black asterisks indicate significance of BMI1 or EZH2 enrichment compared with the IgG control (from cells expressing an NS shRNA); blue asterisks indicate significant differences in BMI1 or EZH2 enrichment in cells expressing a TRIM37 shRNA relative to NS shRNA. Error bars indicate s.d.; $n = 3$ technical replicates of a representative experiment (out of three experiments). **b**, qRT-PCR (top) and immunoblot (bottom) monitoring BMI1 and EZH2 levels in MCF7 cells expressing an NS or TRIM37 shRNA. Error bars indicate s.e.m.; $n = 3$ technical replicates of a representative experiment (out of three experiments). The results indicate that BMI1 and EZH2 levels are unaffected by TRIM37 knockdown in MCF7 cells. **c**, Left, qRT-PCR analysis monitoring expression of two genes that are bound by EZH2 but not TRIM37, *ADAM7* (top) and *YES1* (bottom), after knockdown of TRIM37 or EZH2 in MCF7 cells. Error bars indicate s.e.m.; $n = 3$ technical replicates of a representative experiment (out of three experiments). The results indicate that knockdown of EZH2 but not TRIM37

de-represses *ADAM7* and *YES1* expression. Right, ChIP monitoring EZH2 enrichment at the promoters of *ADAM7* and *YES1* in MCF7 cells expressing an NS or TRIM37 shRNA. Error bars indicate s.d.; $n = 3$ technical replicates of a representative experiment (out of three experiments). The results show that knockdown of TRIM37 has no effect on EZH2 binding at *ADAM7* and *YES1* promoters. Thus, loss of EZH2 binding and de-repression after TRIM37 knockdown is not general to PRC2-bound genes but rather is selective for TRIM37 target genes. **d**, ChIP monitoring H3K27me3 enrichment at promoters of TRIM37 target genes in MCF7 cells expressing an NS or TRIM37 shRNA. Error bars indicate s.d.; $n = 3$ technical replicates of a representative experiment (out of three experiments). **e**, qRT-PCR analysis monitoring BMI1 (left) and EZH2 (right) knockdown efficiency in MCF7 cells after shRNA-mediated knockdown using two unrelated shRNAs against each gene. Expression of each gene was normalized to that obtained with an NS shRNA, which was set to 1. Error bars indicate s.e.m.; $n = 3$ technical replicates of a representative experiment (out of three experiments). **f**, qRT-PCR monitoring TRIM37 target gene expression in MCF7 cells after knockdown of BMI1 or EZH2 using a second shRNA unrelated to that used in Fig. 3h. Error bars indicate s.e.m.; $n = 3$ technical replicates of a representative experiment (out of three experiments). * $P < 0.05$, ** $P < 0.01$.



Extended Data Figure 6 | TRIM37/17q23 copy number and promoter methylation analysis for TRIM37 target genes in human breast cancer samples. **a**, Analysis of 17q23 copy number in a panel of 71 human breast cancer samples; the region corresponding to the *TRIM37* gene is highlighted in yellow. The breast cancer samples shown here are the same as those shown in Fig. 4a. Red indicates increased copy number and green indicates decreased copy number (see Methods). **b**, Promoter methylation analysis. Each of the 60

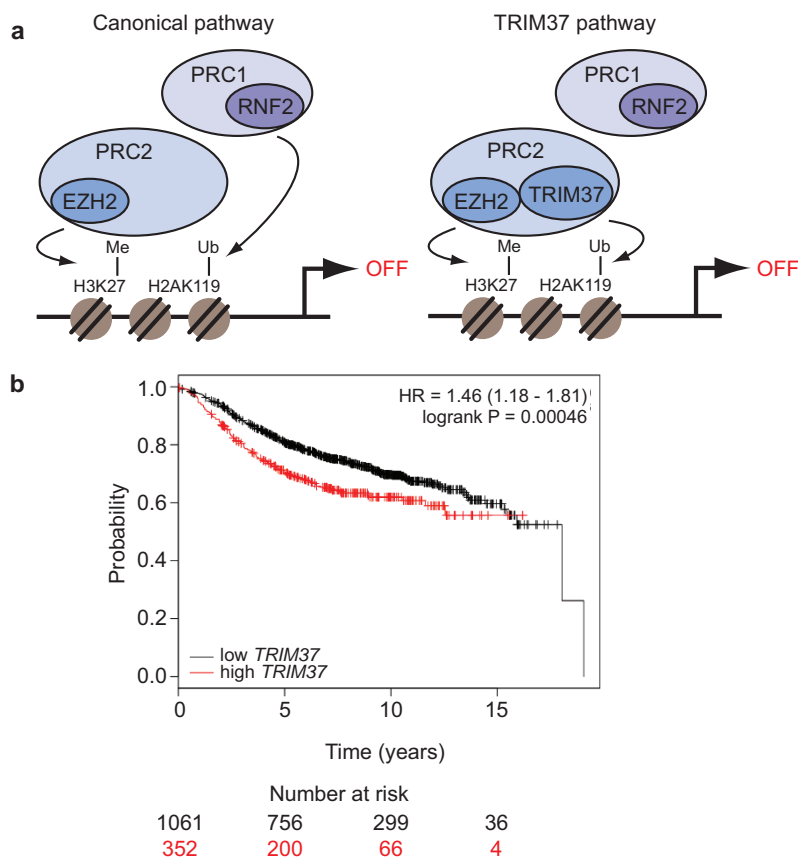
TRIM37 target genes shown in Fig. 4a were analysed for promoter CpG methylation in human breast cancer samples. The level of DNA methylation is shown ranging from low (green) to high (red); white indicates data were not available. The first column is a heat map showing expression of *TRIM37*. The results indicate no significant correlation between *TRIM37* expression and promoter methylation of *TRIM37* target genes.



Extended Data Figure 7 | Control experiments related to Fig. 4.

a, Proliferation of cultured MCF7 cells expressing an NS shRNA or a second *TRIM37* shRNA unrelated to that used in Fig. 4d. Error bars indicate s.d.; $n = 3$ technical replicates of a representative experiment (out of three experiments). **b**, **c**, Tumour formation in mice subcutaneously injected with BT474 (**b**) or FC-IBC02 (**c**) cells expressing an NS or *TRIM37* shRNA. Error bars indicate s.e.m.; $n = 3$ mice per group. **d**, Immunoblot monitoring *TRIM37* levels in NIH 3T3 cells expressing vector, wild-type (WT) *TRIM37* or *TRIM37*(C18R). α -Tubulin (TUBA) was monitored as a loading control. **e**, Immunoblot monitoring *TRIM37* levels in MCF10AT cells expressing vector or Flag-tagged *TRIM37*. **f**, qRT-PCR analysis monitoring knockdown efficiency of a tumour suppression gene in MCF10AT cells expressing the indicated shRNA. The results are given relative to expression after treatment with an NS shRNA, which was set to 1. Error bars indicate s.d.; $n = 3$ technical replicates of a

representative experiment (out of three experiments). **g**, Soft agar assay monitoring colony formation of MCF10AT cells expressing an NS or the indicated shRNA. Error bars indicate s.e.m.; $n = 3$ technical replicates of a representative experiment (out of three experiments). **h**, Tumour formation in mice subcutaneously injected with MCF10AT cells expressing an NS or the indicated shRNA. Error bars indicate s.e.m.; $n = 3$ mice per group. **i**, Soft agar assay monitoring colony formation of MCF10A cells expressing vector or *TRIM37*. Error bars indicate s.e.m.; $n = 3$ technical replicates of a representative experiment (out of three experiments). **j**, Tumour formation in mice subcutaneously injected with MCF10A cells expressing vector or *TRIM37*. Error bars indicate s.e.m.; $n = 3$ mice per group. **k**, Tumour formation in mice subcutaneously injected with BPLER cells expressing vector or *TRIM37*. Error bars indicate s.e.m.; $n = 3$ mice per group. * $P < 0.05$, ** $P < 0.01$.



Extended Data Figure 8 | Schematic model of TRIM37-directed transcriptional repression and Kaplan–Meier analysis comparing survival of breast cancer patients with high or low *TRIM37* expression. **a**, Schematic models for canonical (left) and TRIM37 (right) pathways for target gene silencing. **b**, Kaplan–Meier analysis of survival of patients with low (black) or high (red) *TRIM37* expression. The number of surviving patients at

0-, 5-, 10- and 15-year time points is indicated below the graph. High expression of TRIM37 was significantly correlated with lower survival rate (P value = 0.00046, hazard ratio (HR) = 1.46 with 95% confidence interval 1.18–1.81). The analysis was performed using an online survival analysis tool to analyse the effect of gene expression on breast cancer prognosis using microarray data from 1,809 patients⁴¹.

Extended Data Table 1 | List of catalogue numbers for shRNAs obtained from Open Biosystems/GE Dharmacon or The RNAi Consortium/ Broad Institute

Gene	Catalog number for 1st shRNA	Catalog number for 2nd shRNA
<i>BCL2L10</i>	TRCN0000033595	TRCN0000033596
<i>BMI1</i>	RHS3979-201751271	RHS3979-201751275
<i>CUL1</i>	TRCN0000003391	TRCN0000003392
<i>CUL3</i>	TRCN0000073343	TRCN0000073344
<i>EGR1</i>	TRCN0000013073	TRCN0000013074
<i>EZH2</i>	TRCN0000040074,	TRCN0000040076,
<i>IL24</i>	RHS3979-9607463	RHS3979-9607465
<i>PAWR</i>	TRCN0000058443	TRCN0000058444
<i>PLCB3</i>	TRCN0000020304	TRCN0000020305
<i>PPP1R1B</i>	TRCN0000000434	TRCN0000000433
<i>Rnf2</i> (mouse)	TRCN0000052879	TRCN0000052880
<i>RNF2</i>	TRCN0000040579	TRCN0000040580
<i>SFRP1</i>	RMM3981-201769168	RHS3979-9601103
<i>TP53</i>	TRCN0000062172	TRCN0000062172
<i>Trim37</i> (mouse)*	TRCN0000018866	TRCN0000018869
	TGCTGTTGACAGTGAGCGACCGGGATCAGCACTG- TATATTAGTGAAGCCACAGATGTAATA- TACCAGTGCTGATCCCGGCTGCCTACTGCCTCGGA	TGCTGTTGACAGTGAGCGAGGGATCAGCACTGG- TATATTAGTGAAGCCACAGATGTATA- ATATACCAGTGCTGATCCCGTGCCTACTGCCTCGGA
<i>TRIM37</i> (human)	RHS4430-200178645	RHS4430-200209374
<i>UNC5B</i>	TRCN0000061816	TRCN0000061813

*These shRNAs are no longer commercially available from Open Biosystems/GE Dharmacon, and thus shRNA sequences are provided in lieu of catalogue numbers.

Extended Data Table 2 | List of primers used for quantitative real-time RT-PCR, ChIP and vector construction

	Gene	Forward primer (5' → 3')	Reverse primer (5' → 3')		
qRT-PCR	<i>ACTB</i>	ACGTTGACATCCGTAAGACCT	GCAGTAATCTCCTTCTGCATCC		
	<i>ACTN1</i>	TCCATCGGAGCCGAAGAATC	GTGTCGGTGGATCAAAGCACA		
	<i>ADAM7</i>	GGTGCCGATATGGTCCAAATTA	CCCCAAATTCGGTTCCCTAGTT		
	<i>ASS1</i>	TCCGTGGTTCTGGCCTACA	GGCTTCTCGAAGTCTTCCTT		
	<i>BCL2L10</i>	CGGAAGAAGCGCCATCTCC	AGGCGTCTTCTTCACTTCAG		
	<i>BM1</i>	TTCTGCTGATGCTGCCAATG	TCCGATCCAATCTGTTCTGGTC		
	<i>CDT1</i>	ATGTCAAGGAGCACCACAAG	ACTTTCATCCACGTTGAAGCG		
	<i>CKB</i>	ACAACAACCACATGGCCAAG	AGCCCCACGGTCATGATGAC		
	<i>CUL1</i>	AACAGTGCAAGTGACGATGC	TTGCTCACGCCAATGCTTGG		
	<i>CUL3</i>	TAAACCAACACAGCGGGTTC	TCACCTTGTGGCAGCAAC		
	<i>DDR1</i>	TTCCCCCTTAATGTGCGTAAGG	AGCAGCCGAATGATGTTTGG		
	<i>DNMT1</i>	GAGCTACCACCGCAGACATCA	CGAGGAAGTAGAAGCGTTTG		
	<i>EEF1A1</i>	GAAGACCCACATCAACATCGT	CTCCGCATTTGTAGATGAGGTG		
	<i>EGR1</i>	CAGCACCTTCAACCCTCAGG	GAGATGTCTAGGAAAAGACTGCG		
	<i>EZH2</i>	AGTTCGTGCCCTTGTGTGATG	TGGTGTGCACTGTGCTTTG		
	<i>GAPDH</i>	TGCACCACCACTGCTTAGC	GGCATGGACTGTGGTCATGAG		
	<i>GRIN1</i>	ACGCCATCCTAGTTAGCCATC	GCACGGGTATGCGGTAGAGG		
	<i>HEYL</i>	GGCTGCTTACGTGGCTGTT	GACCCAGGAGTGGTAGAGCAT		
	<i>IL24</i>	TTCTGGGCTGTGAAAGACAC	TTTCTTGCAGAGCTTCTGC		
	<i>IL36A</i>	CCAGACGCTCATAGCAGTCC	AGATGGGTTTCCCTCTGTCTT		
	<i>JPH3</i>	AGAATGGGGATGAGCTCAAAGTC	TTTTGCTACCCGGACATCTC		
	<i>LAMP3</i>	GCGTCCCTGGCCGTAATTT	TGCTTGTCTTAGCTGGTTGCT		
	<i>LTBP3</i>	TCCCCAGGGCTACAAGAGG	AGACACAGCGATAGGAGCCA		
	<i>PARD6G</i>	GTCTCAGACCTTCCGATTCTAC	GGTCCAGAGAGAACCCTTCGGA		
	<i>PARP9</i>	GTGGTTGTGGCCAACTTCTGTG	ACCATGTTCAACCAGCACAAC		
	<i>PAWR</i>	TGATGAAGCAGGGCAGAAAAG	AAACTGTTCTAGGTGGCTCCTG		
	<i>PLCB3</i>	TTCAATTACCCACGGCTTCAAC	TCTTTGCTGTTGCTTTGGCC		
	<i>PPP1R1B</i>	CAAGTCTGAAGAGACCCAAACC	GCCTGGTTCTCATTCAAATTTGCT		
	<i>PROP1</i>	GCCCCAGTGCAGTTGGAACA	TGCTTCCGTTGCTTAGCTCTG		
	<i>P14ARF</i>	CCCTCGTGTGCTGATGCTACTG	ACCTGGTCTTCTAGGAAGCGG		
	<i>RASSF3</i>	GCCTGCAAGCTCTCAGACC	TAGGCTGTGTAGCGCCTCTT		
	<i>RASSF9</i>	GAGGACCTGAGCGAAAAGTAT	TCTGGATGCCACTCAAATGAGA		
	<i>RNF2</i>	GTGCAGACAACCGAACTCA	TTGCCACTTCTAAGGGCTGT		
	<i>SEPN1</i>	CCTGACCCTAGCGAGGAGAC	GGCTGTCCAGTTTTCGGAGG		
	<i>SFN</i>	TGACGACAAGAAGCGCATCAT	GTAGTGAAGACGGAAAAGTTCA		
	<i>SFRP1</i>	TCATGCAGTTCTTCCGGCTTC	TTGTCCAGGGAGGACACAC		
	<i>TBKBP1</i>	GGCGGCTAGAAGAGGCTTTG	CTCCGTCAGCTCGGTGTAG		
	<i>TP53</i>	ACTTGTGCGCTCTTGAAGCTAC	GATCGGGAGAATCTTTGGAACA		
	<i>TRAF2</i>	TGCCCAAGTTCCCTTAAC	TTGCCACAAGTCTTACGCTG		
	<i>TRIM37</i>	AACAGAGCGTGGAGAGCATT	CCTTCTGCCCAACGACAATTT		
	<i>UNC5B</i>	GTCGGACACTGCCAATATAC	CCGCCATTACGTTAGACGAT		
	<i>VCL</i>	AAACTGAACCAGGCCAAAGG	TTTGCCTGCACAGAGTTTAC		
	<i>WNT10B</i>	GTGAGCGAGACCCCACTATG	CACTCTGTAACCTTGCACATCAT		
	<i>YES1</i>	GCCTGTCAAGTGTGAG	AAAGGCGTTACCCCTGAGGAT		
	ChIP	<i>Actb (mouse)</i>	CGAAGCCGGTGTGAGTGAGC	ACCGCCGAGACCCGGCTCC	
		<i>ACTB</i>	CCGTTCCGAAAGTTGCCTT	CGCCGCCGGTTTTATA	
		<i>ADAM7</i>	AACTGGGAGCAAGTGAAGT	CTGCTCCAAGGACACTTTTTTC	
		<i>BCL2L10</i>	AGGAGGTTGTGGTTACAGACC	ACTTAGCAGCCAGAGTATCC	
		<i>CDT1</i>	GGGATTACAGGGCTGAACCA	ATCCGCTCTCTTGGAACTGC	
		<i>CKB</i>	CAGGTGTCCCTTAAGCTGG	CCCTTACGGTTTTGTGGGGT	
<i>CUL1</i>		CGAGGGAGGCTGTAAAACCTG	CGTGGGAAGCTTCTACCTG		
<i>DDR1</i>		ACCTGCTTCTTCTCTGTGC	CCCCAAACGAGAACCCTCAA		
<i>DNMT1</i>		CCACGCTTGGCTAATTTTTG	ATCACGAGGTCTAGGAGTTCTG		
<i>EEF1A</i>		AGCTCGGGATCAAGAATCAC	TGGCCTCTTACGGGTTATG		
<i>EGR1</i>		CTGGGAGTGGAGAGGGAAC	AATCCGAAAGAGGGGCTTCC		
<i>Fas (CP/TSS)</i>		GCCGCTGTGCAGTGGTGA	CTGTGTGTTGGGACGCTCGGG		
<i>Fas (1 kb)</i>		GGCTATAGATCACCTTCAATGTA	GCAGTTAACTCAGGGACCAAG		
<i>Fas (2 kb)</i>		GCGTTGCCATAGCATGAAGT	GAGTTAGGGGACCATAGTCA		
<i>Gapdh (mouse)</i>		CACGCTCGGTGCGTGCC	GCTCAGCCAGTCCAGCC		
<i>GAPDH</i>		TCCGGGTGATGCTTTTCCCTAG	TTTTGGGTGGAAATGTCCTTTTT		
<i>IL24</i>		TTCTTCCGCTGTGGACTACTGTG	AACAACACAGAGGTTGCTTGG		
<i>IL36A</i>		TCAACTATGTGTGGCTTGTGC	GCTAAACTCATTCCACAAGAAGC		
<i>JPH3</i>		GTTTGCAAAGGGCCTCAGTC	AGGAACTGCGTCATGGGAAG		
<i>LAMP3</i>		AGCACCTGGACAGCAATTAC	AGGTCAGGTTGTGAGGTGAATG		
<i>PARP9</i>		GTGTGGTTCTGGCTAAATGCAC	TGCGGCACATTTGTACAAGG		
<i>PAWR</i>		TGTTGTGGGAACGATATGGC	TTAGGTAACACGCGCTCAGC		
<i>PLCB3</i>		TGTGAAGGTCTCCAGCCATG	ATGGGAACTGGACAGGAATCTG		
<i>RASSF3</i>		TAATCCAGCTACTTGGGAAGC	TTTTGCTCTGTCAACCAGAC		
<i>RASSF9</i>		ATCATCGCCACCTGGTATCAC	GCAAACAGAGGGAAACAACATGG		
<i>SEPN1</i>		AGGCGCAGTGTATGTGTAC	TGGGAGGAAGGAAATGACAGAC		
<i>SFN</i>		ACAGGCCACCAACTTGAAGG	TAACAAGCAGCCTCTGAAGC		
<i>SFRP1</i>		CCCTCCACCTCAAGCCAAAT	ACAAGTCTCTGCTGCCATTG		
<i>TP53</i>		TTGCCAGGAAAGATGCACAG	ATGTGGCAGTTGTGTTGCTC		
<i>TRAF2</i>		GCGCGCTCTTTGAGGAAAAA	CAGCCCTCAGGAAGCTGTAG		
<i>WNT10B</i>		TTCTTCTGCCTCCACACTCTC	AGCACTTCTCGGAAACCTG		
<i>YES1</i>		TGATGAGGGTGTGAGTAACGC	TGTTGGCTGTTTCTCTCTC		
GAL4 recruitment		<i>GAL4-UAS</i>	GACACTATAGAATCGAGCAGCTG	ATGAATTCGAGCTCGGTACCC	
		<i>TRIM37</i>	AACAGAGCGTGGAGAGCATT	CTTCTGCCCAACGACAATTT	
		Vector construction	<i>TRIM37-C18R</i>	CATACGATGAAACATCGGAAAACCTCAGC	CATACGATGGAAGAAATTCGGGGATG
			<i>H2A-KKRR (N terminus)</i>	ATGTCTGTGCTGGGAAACCA	ATGCGCGTCTCTCTGTTGTC
			<i>H2A-KKRR (C terminus)</i>	(P)-CATCCCTCGTCACTCCAG	TGGTGGCTCTAAAAGAGCC
			<i>Cloning TRIM37 into pGEX4T-1</i>	GAATTCATGGATGAACAGAGCGTGGA	GCGGCCGCTCTTCCACTATTTT
			<i>Cloning TRIM37 into pCMX-Gal4</i>	GGTACCAAAATGGATGAACAGAGCGTGGA	GCTAGCTCTTCCACTATTTT
			<i>TRIM37ΔRING</i>	GAATTCATGGATGAACAGAGCGTGGAACCTCCAGC-TACGAGAAGTGTAA	CTCCAGCTACGAGAAGTGTAA
			<i>TRIM37ΔBBOX</i>	(P)-ATGTTTGGTGAGACTGCAGAG	ATTTATGACGAACAGCTCACTAAA
			<i>TRIM37ΔCC</i>	(P)-AGTGACGTGTTGCTCATAAATTTCT	GAGTTGATATCTAAGAGCTCAGAGA
<i>TRIM37ΔMATH</i>			(P)-AGTAGCTGAATCGTAAGATGGCA	GCAAATGAAGGATACTTGAATCCACA	
<i>TRIM37ΔNLS</i>			(P)-CAAGCCACTGAAAAGTCAACC	ATGTCACCTTGGGGGCTAAT	